Journal of the European Ceramic Society **19** (1999) 1801–1826

PII: S0955-2219(99)00009-6
0955-2219/99/$ - see front matter

REVIEW

Bismuth Based Oxide Electrolytes—Structure and Ionic Conductivity

N. M. Sammes,[a]* G. A. Tompsett,[b] H. Näfe[a] and F. Aldinger[a]

[a]Max Planck Institut für Metallforschung, Pulvermetallurgisches Laboratorium, Heisenberg Straße 5, D-70569, Stuttgart, Germany
[b]Department of Technology, University of Waikato, Private Bag 3105, Hamilton, New Zealand.

(Received 23 September 1998; accepted 12 December 1998)

Abstract

Bismuth oxide systems exhibit high oxide ion conductivity and have been proposed as good electrolyte materials for applications such as solid oxide fuel cells and oxygen sensors. However, due to their instability under conditions of low oxygen partial pressures there has been difficulty in developing these materials as alternative electrolyte materials compared to the state-of-the-art cubic stabilised zirconia electrolyte. Bismuth oxide and doped bismuth oxide systems exhibit a complex array of structures and properties depending upon the dopant concentration, temperature and atmosphere. In this paper we comprehensively review the structures, thermal expansion, phase transitions, electrical conductivity and stability of bismuth oxide and doped bismuth oxide systems. © *1999 Elsevier Science Limited. All rights reserved*

Keywords: bismuth oxide, ionic conductivity, fuel cells, sensors, thermal expansion.

1 Introduction

The major component of an electrochemical cell is the electrolyte, which is the ionically conducting membrane that separates the two electrodes. At present electrolyte materials used in electrochemical devices are based on doped zirconia systems which typical operate at temperatures above 900°C. Yttria stabilised zirconia, YSZ ($Zr_{1-x}Y_xO_{2-x/2}$) is a typical electrolyte material which exhibits a high oxygen ion conductivity at high temperatures and is stable under reducing atmospheres. However, electrolytes based on zirconia have a low ionic conductivity compared to bismuth oxide based electrolytes at comparable temperatures. For example δ-Bi_2O_3 is 1–2 orders of magnitude higher conductivity than YSZ. Replacement of YSZ with an intermediate-temperature oxide ion conductor, in for example solid oxide fuel cells, would give a significant reduction in the material and fabrication problems together with an improvement in the efficiency and longevity of the cell. The search for a suitable intermediate temperature electrolyte based on bismuth oxide has been carried out over many years.

The aim of this paper is to comprehensively review the literature on the properties of oxide ion conducting electrolytes based on bismuth oxide. The properties of structure and conductivity are described for these systems.

*To whom correspondence should be addressed now at: Department of Technology, The University of Waikato, Hamilton, New Zealand (supported by an Alexander von Humboldt Fellowship). Tel.: +64-7-838-4065; fax: +64-7-838-4835; e-mail: nsammes@waikato.ac.nz

2 Pure Bi_2O_3

2.1 Structure

The work was reviewed prior to 1964 by Levin and Roth, and has been the subject of a number of investigations for almost 100 years.[2–12] Four polymorphs of Bi_2O_3 have been reported in the literature, viz: α, β, γ and δ-phases.

The phase transition from the monoclinic α-phase, to the high temperature cubic δ-phase, at approximately 730°C, has been observed by a number of authors[1,6,8,9]. The δ-phase was also found to be stable up to its melting point of approximately 825°C.[1–12] The data regarding the enthalpy of the α to δ phases are, however, inconsistent;[6,8,9,13,14] in fact the extremely large value given by Gattow and Schroder of 28 kcal mol^{-1} has been shown to be incorrect, since it is based on contradictory information;[3,6,14] a

value of 7·06 kcal mol^{-1} is considered as correct, even though it is still 2·7 times the heat of fusion.[15] The results for the transition temperatures have been found, therefore, to also be somewhat contradictory. In fact, the values for the transition of α to δ have varied from 717[6] to 740°C.[8] The more recent work of Harwig and Gerards,[15] who showed that the transition occurred at 729–730°C, is generally now accepted as the transition temperature.

On cooling from the high temperature δ-phase to room temperature, a large hysteresis has been observed, with the possible occurrence of two intermediate metastable phases[8–11] viz: the tetragonal β-phase[4,5,8] or the bcc γ-phase.[1–5] The tetragonal β-phase occurs at approximately 650°C on cooling, while the γ-phase is formed at approximately 640°C. The γ-phase has also been shown to persist to room temperature, when the cooling rate is kept very low.[15] The β-phase, however, has not been stabilised to room temperature but instead decomposes to the α-phase. Table 1 summarises the transition temperatures, observed by a number of authors, for the transitions of Bi_2O_3.

2.2 The structure of α-Bi_2O_3

The crystal structure was first determined by Sillen,[4,16,17] from Wissenberg photographs. The Bi positions were determined from Patterson analysis, and the possible oxygen positions were given from the space considerations. Malmos,[18] using single crystal X-ray diffraction, determined more information regarding the oxygen positions, and confirmed the positions of the bismuth atoms, and two of the oxygen atoms observed by Sillen. However, one of the oxygen atoms was found to be in a different position to that observed by Sillen. Later work by Harwig and Gerards,[15] using high temperature powder X-ray diffraction, agreed with the findings of Malmos,[18] and confirmed the cell to be monoclinic, with cell parameters $a = 5{\cdot}8486(5)$ Å, $b = 8{\cdot}166(1)$ Å, $c = 7{\cdot}5097(8)$ Å, and $\beta = 113{\cdot}00(1)°$. Later work by Harwig,[19] using neutron diffraction, confirmed the cell dimensions to be $a = 8{\cdot}8496(3)$ Å, $b = 8{\cdot}1648(4)$ Å, $c = 7{\cdot}5101(4)$ Å, and $\beta = 112{\cdot}977(3)°$, and that the spacegroup was $P2_{1/c}$ (b as an unique axis). The atomic co-ordinates for α-Bi_2O_3 have also been determined by Harwig,[19] Malmos[18] (using single crystal X-ray diffraction), Malmos and Thomas[20] (powder X-ray diffraction), and Cheetham and Taylor[21] (Neutron diffraction). The α-Bi_2O_3 structure consists of layers of bismuth atoms parallel to the (100) plane of the monoclinic cell, separated by layers of oxide ions. Strings of voids were shown to be present in the oxygen sheets in the direction of the c-axis.[19,22]

2.3 The structure of δ-Bi_2O_3

The monoclinic to cubic phase transition ($\alpha - \delta$) occurs at approximately 730°C, as described above. δ-Phase is stable from this temperature until the melting point of Bi_2O_3 at approximately 825°C. Sillen reported that the structure of Bi_2O_3, using powder X-ray diffraction on quenched samples, was a simple cubic phase. The simple cubic structure was shown to be related to the fluorite structure, but with ordered defects in the oxygen sub-lattice in the direction. Gattow and Schroder showed, using high temperature powder X-ray diffraction, that δ-Bi_2O_3 crystallises in the space group Fm-3m.

Gattow and Schroder[6] also showed that the system belongs to the CaF_2-type structure, and has an oxygen-defective lattice, although they rejected the ordered defect sub-lattice described by Sillen[4], and preferred to describe the system as one in which 75% of the oxygen sub-lattice sites are filled. The system can be described by the simple Fm-3m space group.

The high ionic conductivity in δ-Bi_2O_3 supports the view that there is an average occupation of oxide ions in the oxygen lattice sites, which can move from site to site through the bismuth sub-lattice. Willis, using neutron diffraction studies, showed that the CaF_2[23], UO_2[24] and ThO_2[24] systems could not be described by the ideal fluorite structure. The author explained that a better description of his data assumed that the fluorine atoms are displaced slightly towards the centres of the interstices, which surround each fluorine tetrahedrally. Since there is a high degree of disorder in δ-Bi_2O_3, this model could be used to describe its structure. Figure 1 shows a diagrammatic representation of the fluorite-related models for δ-Bi_2O_3.

Table 1. Bi_2O_3 phase transition temperatures reported the literature

Transition	*Levin and McDaniel*[13]	*Gattow and Schroder*[6]	*Gattow and Schutze*[8]	*Levin and McDaniel*[12]	*Rao et al.*[9]	*Harwig and Gerards*[15] *(DTA)*	*Harwig and Gerards*[15] *(TGA)*
$\alpha \rightarrow \delta$	–	717	710–740	730	727	729	730
$\delta \rightarrow L$	825	824	842	825	–	824	–
$\delta \rightarrow \beta$	–	–	660–640	–	630	650	649
$\beta \rightarrow \delta$	–	–	–	–	–	662	667
$\beta \rightarrow \alpha$	–	–	640–430		543	652–534	576–497
$\delta \rightarrow \gamma$	–	–	–	–	–	639	643
$\gamma \rightarrow \delta$	–	–	–	–	–	663	652
$\gamma \rightarrow \alpha$	–	–	–	–	–	639–543	604–562

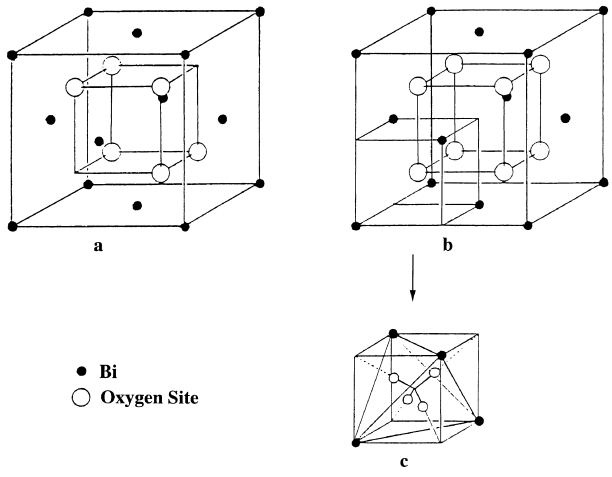

Fig. 1. Structure models for δ-Bi_2O_3 (Ref. 19); (a) Sillen model showing ordered defects in the $<111>$ direction; (b) Gattow model: average distribution of 6 oxygen atoms about the sites (Sc) of Fm3m (xxx, $x=1/4$); (c) Willis model: average distribution of 6 oxygen atoms about the sites (32f) of Fm3m (xxx, $x=1/4+\delta$).

Verkerk and Burggraaf,[25] using neutron diffraction on $(Bi_2O_3)_{0.8}(Er_2O_3)_{0.2}$, showed that the Sillen[17] model was less satisfactory than the Gattow and Schroder[6] or Willis[23] models in describing the structure of δ-Bi_2O_3; they concluded that there is no long range $<111>$ ordering of vacancies. However, Zav′yalova and Imamov,[26] using electron diffraction studies, and later, Madernach and Snyder[27] using calculations, showed that the vacancies are ordered in the $<111>$ direction, although the diffraction patterns would have a very low intensity. Other models to describe the δ-Bi_2O_3 structure have been proposed by Kilner and Faktor,[28] who describe a $<110>$ arrangement of vacancies in small completely regular domains (see Fig. 1). Jacobs and Mac Donaill,[29] using computer simulations, showed that an ordered array of oxygen vacancies, in δ-Bi_2O_3, aligned along the $<111>$ planes, as described by Sillen,[17] are more stable than vacancy arrays aligned along $<110>$ or $<100>$. However, Jacobs and Mac Donaill[29] also showed that defects aligned along $<110>$ are present in large numbers, and can be described by a disordered Sillen model. Jacobs and Mac Donaill,[30–32] looked at a number of models to describe the disorder and high oxygen ion conductivity in δ-Bi_2O_3 and used computational simulations to investigate the models.

2.4 The structure of β and γ-Bi_2O_3

The transition to the metastable β-Bi_2O_3, on cooling from the high temperature δ-phase (or from the liquid phase), can occur at approximately 650°C[15] as described in Fig. 2.[33] Harwig and Gerards[15] have shown, using high temperature X-ray diffraction, that the β-phase is tetragonal, with cell dimensions $a=7{\cdot}738(3)$ Å, and $c=5{\cdot}731(8)$ Å, at

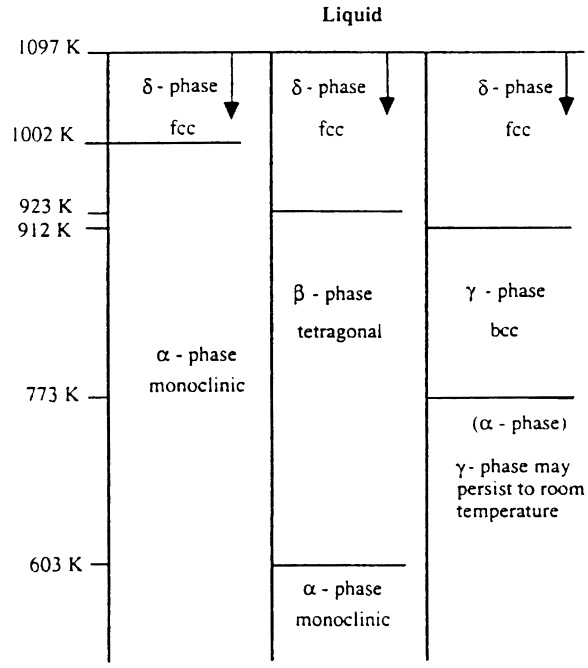

Fig. 2. The stable and metastable regions found in Bi_2O_3 (Ref. 33).

643°C. Further work by Harwig[19] revealed that the voids in the oxygen sublattice of the structure were ordered in the (001) direction.

A transition to a metastable bcc phase is also possible on cooling δ-Bi_2O_3, or from the melt, to 639°C.[15] This phase is known as γ-Bi_2O_3, and can persist down to room temperature. Harwig[19] showed that γ-Bi_2O_3 had a cell dimension of 10·268(1) Å at room temperature, which was also in agreement with the work of Levin and Roth.[1] The authors also found that γ-Bi_2O_3 was isomorphous with the system $Bi_{12}GeO_{20}$.

2.5 Thermal expansion of α, β, γ and δ-Bi_2O_3

The thermal expansion coefficients were first examined by Gattow and Schroder[6] who found a very high value of $43{\cdot}6\times10^{-6}$ °C^{-1} for δ-Bi_2O_3. Levin and Roth[1] found a value that was half as large as that found by Gattow and Schroder. The typical values of the thermal expansion coefficients have been summarised in Table 2.

The thermal expansion data is a very important value to realise, particularly when fabricating electrochemical devices from it, as it may impact on the heating and cooling characteristics of that device. In fact, it is quite apparent from Table 2 that the transition from δ-Bi_2O_3 to β-Bi_2O_3 is accompanied by a large volume change, and thus the mechanical integrity of the material would be suspect.

2.6 The electrical properties of Bi_2O_3

Mansfield,[36] and later Hauffe and Peters[37] examined α-Bi_2O_3, and observed *p*-type conductivity at room temperature, which transformed into *n*-type

Table 2. Thermal expansion coefficients for Bi_2O_3

Temperature (°C)	*Expansion coefficients (10^{-6}/°C)*				*Reference*
	α	β	γ	δ	
100–200	12·2	–	–	–	6
200–400	12·4	–	–	–	6
400–575	14·2	–	–	–	6
575–675	14·8	–	–	–	6
675–750	–	–	–	43·6	6
Room temp.	–	–	–	22·6/22·5	34/35
25–730	11·0		–	–	1
730–825	–	23·0	–	–	1
640–25	–	–	20·0	–	1
650–500	–	–	–	24·0	1

at approximately 550°C and at oxygen partial pressures below $1{\cdot}3\times10^{-5}$ atm. Rao *et al.*[9] suggested that the *n*-type conduction occurs above 650°C, even in air. They explained their findings in terms of the band model, where the Fermi level moves upward with increasing temperature, accompanying the loss of oxygen from the lattice. They went on to describe that the increase in conductivity from α-Bi_2O_3 to δ-Bi_2O_3 was due to a large broadening of the bands. Takahashi *et al.*, [38] however, reported that in δ-Bi_2O_3 oxygen ions were the majority charge carrier, with an increase of over a factor of 3 being observed from the low temperature α-phase to the high temperature δ-phase.

Later, Harwig and Gerards[39] systematically measured the conductivities of α, β, γ and δ-phases of Bi_2O_3. Figure 3 shows some typical plots of conductivity versus temperature for Bi_2O_3, during repeated heating and cooling runs. The conductivity was found to increase 3 orders of magnitude at the α to δ transition at 729°C; in fact the highly disordered state (approximately 75% of the liquid state) reached in δ-Bi_2O_3 accounts for the high conductivity. In the cooling direction, a hysteresis of 80–90°C was observed which preceded the transition to either the β or γ-phases, as described above. Harwig and Gerards[39] and later Shuk and Mobius[40] described that the conductivity in the β, γ, and δ-phases is mainly ionic, with oxide ions being the main charge carrier. The δ-phase was found to be up to 3 orders of magnitude greater than the two intermediate phases. The conductivity of the δ-phase was also found to be independent of the oxygen partial pressure, at least down to 10^{-3} Pa. The α-phase, however, varied with oxygen partial pressure $PO_2^{1/4}$, and thus it can be concluded that holes are the majority charge carrier.

Mairesse[41] has recently summarised the reasons for the relatively high oxygen ion conductivity in δ-Bi_2O_3 as:

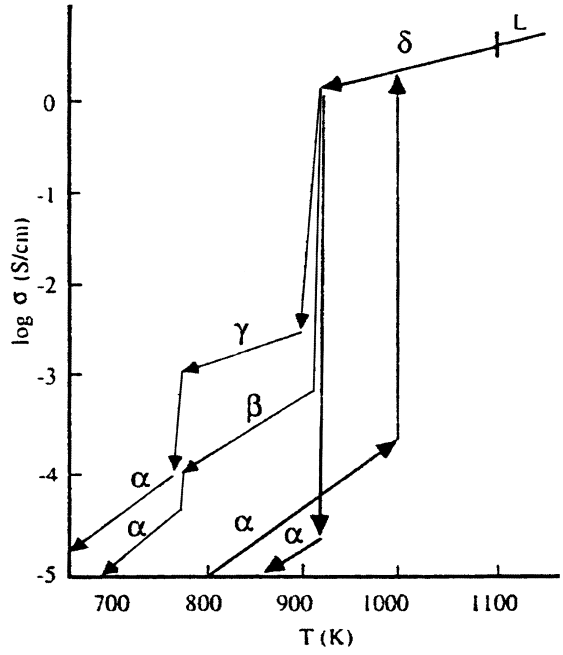

Fig. 3. Electrical conductivity of Bi_2O_3 as a function of temperature (Ref. 33).

(i) 1/4 of the oxygen sites are vacant in the fluorite-type lattice;
(ii) the electronic structure of Bi^{3+} is characterised by the presence of $6s^2$ lone pair electrons, leading to high polarisability of the cation network, which in turn leads to oxide ion mobility;
(iii) the ability of the Bi^{3+} to accommodate highly disordered surroundings.

The conductivities of the phases are summarised in Table 3.[42]

The structure of the high temperature δ-Bi_2O_3 has been examined recently using EXAFS,[35,43–45] and has shown that most of the oxide ions are displaced from the tetrahedral sites and are situated nearly at the triangular centres of a Bi-tetrahedra, and the amount of displacement becomes larger with increasing temperature.

3 Doped Bi_2O_3 Systems

3.1 Bi_2O_3–M_2O_3 (where $M = Y$ or rare earth oxide)

Most of the solid solutions of Bi_2O_3–M_2O_3, that are used as ionic conductors, are based on either the fcc δ-Bi_2O_3 form (such as found in Bi_2O_3–Y_2O_3), or the rhombohedral structures (such as that found in Bi_2O_3–La_2O_3). The type of structure formed depends on the dopant type (primarily the ionic radius of the dopant) and the concentration. The system Bi_2O_3–Gd_2O_3 belongs to both the fcc and rhombohedral phases, which are very good ionic conductors. In general, it is found that the

Table 3. Conductivity parameters observed for Bi_2O_3phases

Phase	*Existence domain (°C)*	*Conductivity at 600°C (Scm^{-1})*	*Conductivity at 650°C (Scm^{-1})*
α-Bi_2O_3	0–730	ca. 10^{-4}	ca. 3×10^{-4}
β-Bi_2O_3	648 down to 500 500 down to 663	ca. 10^{-3}	ca. 2×10^{-3}
γ-Bi_2O_3	650 down to 600	ca. 3×10^{-3}	ca. 5×10^{-3}
δ-Bi_2O_3	Greater than 730	N/a	ca. 1

rhombohedral phase is formed in the case of relatively large M^{3+} ion, and the fcc structures are usually formed in the case of a relatively small cation radius. The lanthanide elements increase in cationic radii from 0·97 Å for Lu^{3+} to 1·18 Å for La^{3+}.[47] Iwahara et. al[46] showed the regions of the rhombohedral and fcc phases present in M_2O_3–Bi_2O_3 system, and are shown in Fig. 4.

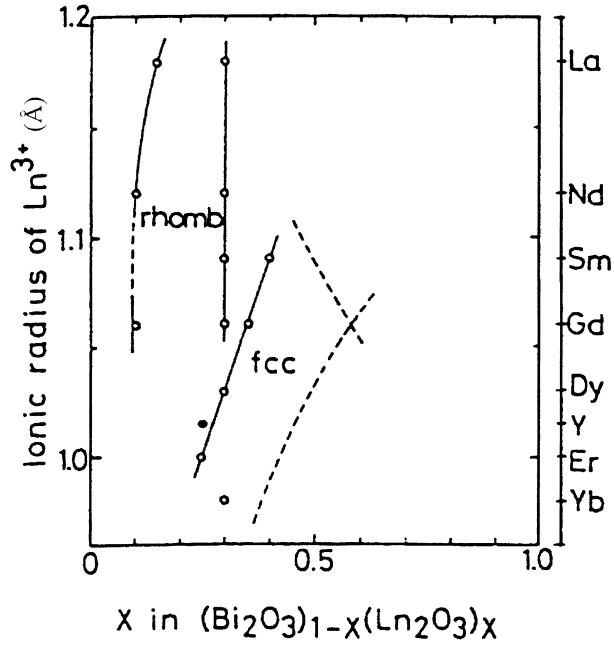

Fig. 4. Formation range of the rhombohedral and fcc phases in the ionic radius of Ln^{3+} versus composition diagram; rhomb = rhombohedral, and fcc = face centred cubic, in relation to δ-Bi_2O_3 (Ref. 46).

3.2 Bi_2O_3–Y_2O_3

Datta and Meehan[48] reported that the system Bi_2O_3–Y_2O_3 showed a fcc solid solution, whose structure was related to the defect fluorite-type and was stable over a wide range of temperatures. The phase that is formed is related to the high temperature modification of Bi_2O_3, and is sometimes designated δ^*. Both δ and δ^* crystallise in apparently the same fcc structure, and due to its highly defective nature, contains a large concentration of intrinsic oxygen vacancies.[4,49] Thus, from this preliminary work, stabilisation of the high temperature δ-phase to low temperatures is very effective, and has thus been studied by a number of groups.[50–59] Datta and Meehan[48] studied the phase equilibrium diagram of Bi_2O_3–Y_2O_3 and showed that samples containing 25 mol% Y_2O_3 formed the stable δ-phase at temperatures below 400°C. The original phase equilibrium diagram given by Datta and Meehan is shown in Fig. 5. The authors suggested that at 25 mol% Y_2O_3, a compound, Bi_3YO_6 is formed which has an fcc structure, stable to room temperature. However, the later work of Watanabe and co-workers,[57,60] suggested that the phase diagram proposed by Datta and Meehan did not show the equilibrium state, because the fcc phase is the high temperature modification, in much the same way as that of the intrinsic δ-Bi_2O_3. Watanabe and Kikuchi[57] identified a hexagonal phase with a layered structure as the low temperature modification, which converts to the fcc structure at approximately 720°C. The system also has a very narrow solid solution range of between 21·5 and 23·5 mol% Y_2O_3 at 650°C. Watanabe[60] went on to suggest that the hexagonal layered structure of the low temperature stable phase is isomorphous to the alkaline earth-doped Bi_2O_3 systems. It was

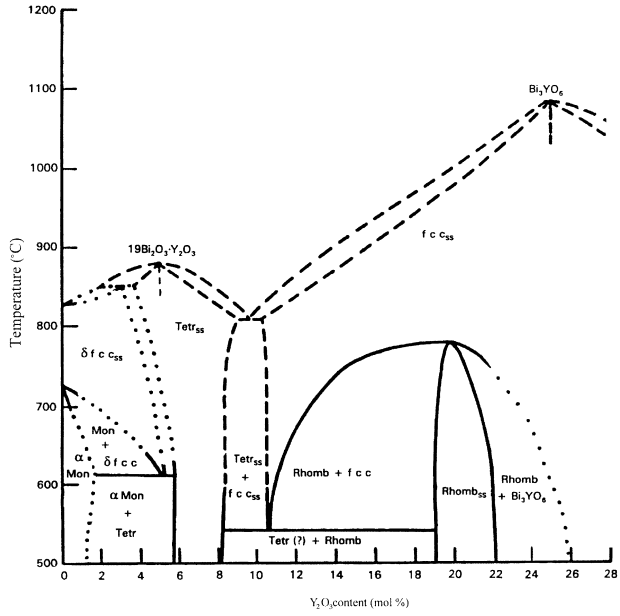

Fig. 5. Phase equilibrium diagram for the system Bi_2O_3–Y_2O_3 (Ref. 83).

also suggested that the formation of the hexagonal layered structure is what gives the material its good ionic conductivity properties.[61] Another phase that was recently found was that of a triclinic structure which formed a solid solution with a composition of 47·5 – 49 mol% Y_2O_3. The triclinic structure is based on pseudo-fcc subcells and transforms into the δ-form at 1010°C. Hence, Watanabe[62] suggested that the formation of the hexagonal and triclinic forms imply that the Y_2O_3-stabilised δ-phase is no more than a quenched-in metastable

high temperature form. Thus, the author re-examined the phase equilibrium diagram and proposed that shown in Fig. 6 to be the correct form of the Bi_2O_3–Y_2O_3 phase equilibrium diagram. In fact he proposed 4 low temperature stable intermediate phases; at 21·5–24 mol% Y_2O_3, 31·5–35 mol% Y_2O_3, 47·5–49 mol% Y_2O_3, and 57–58 mol% Y_2O_3. Kruidhof *et al.*[58] investigated the thermodynamic stability of Bi_2O_3 containing 22–32·5 mol%, and suggested that solid solutions containing less than 31·8 mol% Y_2O_3 had the fcc structure and were metastable below 840°C. The authors observed a sluggish transformation from cubic to hexagonal, when annealed at 650°C. The hexagonal phase was also observed to decompose into the fcc structure above 740°C.

Takahashi and co-workers,[50,63–65] demonstrated that high ionic conductivity can occur in Y_2O_3-doped Bi_2O_3 due to the stabilisation of the high temperature δ-phase to lower temperatures. They found a stability range of 25 – 43 mol%. The ionic conductivity of $(Bi_2O_3)_{1-x}(Y_2O_3)_x$ was thoroughly examined by Takahashi *et al.*,[50,51] and the data is summarised in Fig. 7. There are a number of issues that can be raised from the plots. Firstly, the ionic conductivity of Bi_2O_3 doped with more than 25 mol% Y_2O_3 does not go through the same transition as observed in pure Bi_2O_3, and thus does not show a jump in conductivity with increasing temperature. However, samples containing less than 25 mol% Y_2O_3 show an abrupt increase in the conductivity, due to a phase transition. Secondly, samples containing less than 25 mol% Y_2O_3 showed a significant hysteresis, with a difference of between 50 and 100°C observed between the heating and cooling cycles.

The phase transition observed in samples containing less than 25 mol% Y_2O_3 was discussed by Takahashi *et al.*,[50] however, they did not ascribe a phase relation nor did they give any crystallographic data of the lower temperature phase. Thus, it was not until the work of Watanabe and Kikuchi,[57] and later Watanbe,[60] that the low temperature phase was found to be hexagonal. Dordor *et al.*[61] examined the low temperature hexagonal phase, $Bi_{1.55}Y_{0.45}O_3$, and looked at the ionic conductivity, as showed in Fig. 8. As described above, many previous authors considered that the δ-phase was stable to room temperature, however, as was shown by Watanabe and co-workers, the δ-phase was only metastable, and was really only a quenched-in phase which slowly converted to the hexagonal phase. However, what Watanabe also showed was that the conductivity of the hexagonal phase is approximately 1 order of magnitude lower than that of the metastable phase.

As has already been explained, δ-Bi_2O_3 has a defective fluorite structure in which 43% of the regular anion sites are randomly occupied, and the remaining 1·28 oxygen's per unit cell are displaced from their ideal positions along the < 111 > axis. It

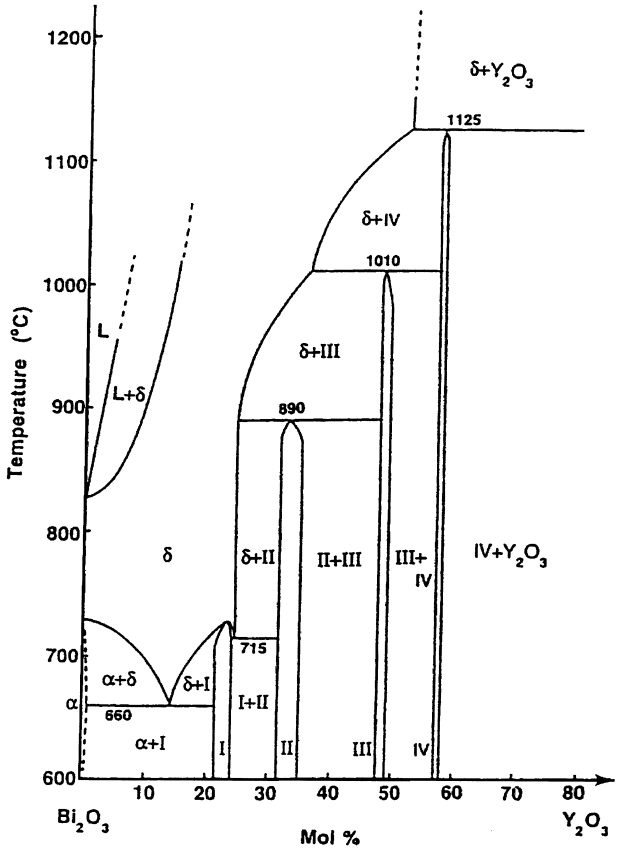

Fig. 6. Alternative phase relations in the system Bi_2O_3–Y_2O_3. I, II, III, and IV represent the low temperature stable intermediate phases with the composition of $x = 0{\cdot}215$-$0{\cdot}24$, $0{\cdot}315$–$0{\cdot}35$, $0{\cdot}475$–$0{\cdot}49$, and $0{\cdot}57$–$0{\cdot}58$ respectively, in $Bi_{1-x}Y_x\ O_{1{\cdot}5}$, L = liquid, $\alpha = \alpha$-Bi_2O_3 and $\delta = \delta$-Bi_2O_3 (Ref. 62).

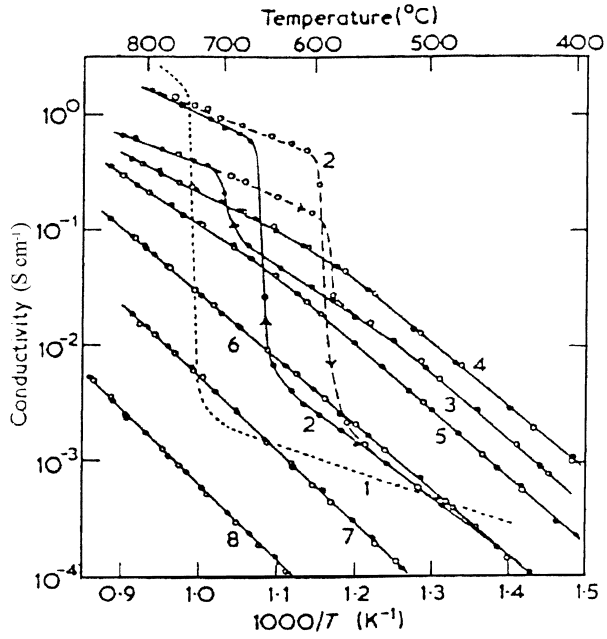

Fig. 7. Conductivity of $(Bi_2O_3)_{1-x}(Y_2O_3)_x$ in air; the values for x are 1 = 0, 2 = 0·05, 3 = 0·2, 4 = 0·25, 5 = 0·33, 6 = 0·425, 7 = 0·5, 8 = 0·6 (Ref. 51).

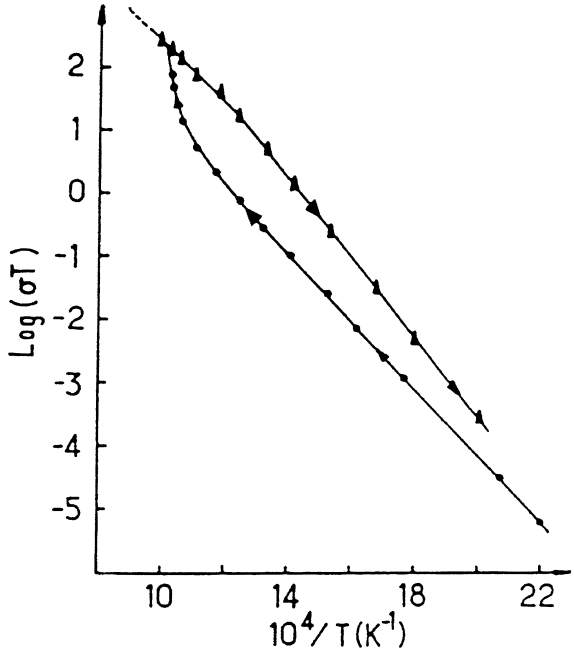

Fig. 8. Temperature dependence of the bulk conductivity of the polymorphs of $Bi_{1.55}Y_{0.45}O_3$; filled circles = hexagonal phase, filled triangles = cubic phase (Ref. 61).

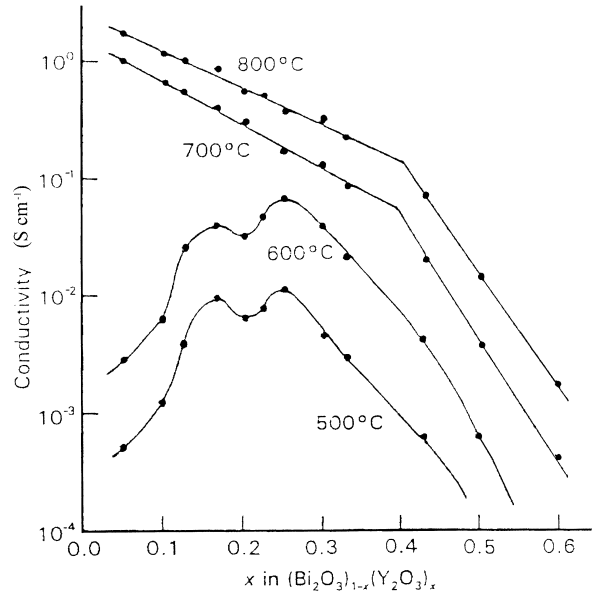

Fig. 9. Oxide ion conductivity isotherms of $(Bi_2O_3)_{1-x}(Y_2O_3)_x$ in air, as a function of temperature (Ref. 50).

has, thus, been observed by Battle *et al.*,[66,67] using Bragg and diffuse neutron scattering studies, that in $(Bi_2O_3)_{1-x}(Y_2O_3)_x$ the number of $<111>$ displaced anions decreases when Y^{3+} is introduced, and decreases with increasing Y^{3+}, although the extent of short range ordering on the anion sublattice was found to increase. The authors also suggested that Y^{3+} stabilises the fluorite structure by ordering the vacancies on the oxygen sublattice in chains along the $<111>$ and $<110>$ directions. Infante *et al.*,[68] using powder neutron diffraction, suggest that most of the oxygen's in the lattice (78%) are in sites displaced 0·335 Å along directions from the normal fluorite positions, while a smaller number (22%) are displaced 0·80 Å along $<111>$ directions, and that no oxygen remains in normal positions. They also suggested that a smaller displacement occurs along the $<111>$ direction, of 0·25 Å, for the cations.

Takahashi *et al.*[50] described the effect of temperature on the conductivity maximum between 500 and 700°C, as seen in Fig. 9. What was observed is that at lower temperatures, the conductivity exhibits 2 maxima, where the conductivity of 25 mol% Y_2O_3-doped Bi_2O_3 at 500°C, is greater than that of 17 mol% Y_2O_3-doped Bi_2O_3. The second maxima was described as being due to the lower limit at which the fcc phase is stabilised, however, the first maxima has not been fully explained, although it has been postulated as being due to the lowest content of the Y^{3+} ion within the range of the single-phase solid solution formation; $x = 0{\cdot}17$–$0{\cdot}25$ in $(Bi_2O_3)_{1-x}(Y_2O_3)_x$.

Takahashi *et al.*[53] Verkerk and Burggraaf,[25,52] showed that the equilibrium partial pressure of stabilised Bi_2O_3 is quite low; at 900 K, for example, it was shown to be 10^{-12} atm. In fact they suggested that the material could be reduced to metallic Bi metal. However, later work by Jurado *et al.*,[69] Wang *et al.*[55] and Duran *et al.*[70] showed that the oxygen partial pressure stability range was much greater. Figure 10 shows that the dependence of the conductivity on oxygen partial pressure for $(Bi_2O_3)_{0.70}(Y_2O_3)_{0.30}$ was constant to below 10^{-14} atm, $(Bi_2O_3)^{0.725}$ $(Y_2O_3)_{0.275}$ was found to be stable to below 10^{-20} atms, with negligible hole or electron conductivity. Now, the partial pressure of oxygen for Bi/Bi_2O_3 equilibrium is of the order of 10^{-13} atm; this value may be a little higher for stabilised Bi_2O_3, however not enough for the very low partial pressures observed above. Wachsman *et al.*[72] tried to explain this discrepancy using ac conductivity, and found that the doped sample (in this case Er_2O_3-doped Bi_2O_3) was stable to oxygen partial pressures lower than 10^{-20} atm, using a zirconia oxygen pump to obtain the oxygen partial pressures. However, when the authors annealed the sample in H_2/H_2O (10^{-21} atm O_2), or used H_2/H_2O to obtain the oxygen partial pressures, they found that Bi metal was formed. They showed that the differences were due to kinetic versus thermodynamic stability. Thus, they explained, that when a fuel, such as H_2, is present, reduction is observed, and that the stability in the absence of H_2 is due to slow heterogeneous kinetics. This does not, however, explain the findings of Wang *et al.*[55] and Jurado *et al.*[69] who used H_2/H_2O mixtures in their experiments.

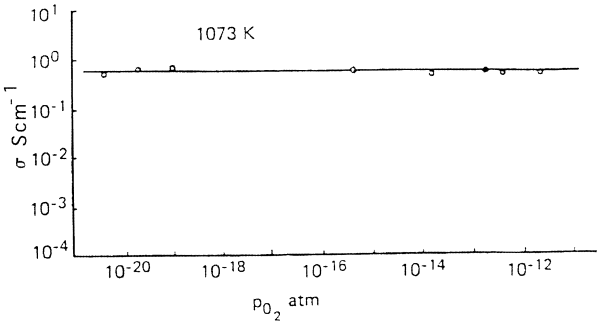

Fig. 10. Dependence of the conductivity on oxygen partial pressure for $(Bi_2O_3)_{0.725}(Y_2O_3)_{0.275}$ at constant temperature (Ref. 55).

Whatever the reasons, a lot of work has been undertaken to reduce the effect of H_2 on the sample, particularly in relation to solid oxide fuel cell systems. These have included using a double layer of zirconia/stabilised bismuth oxide,[73] where the zirconia-coated side is exposed to the fuel gas, and the use of double-stabilisers.[74–76] Doped-bismuth oxide systems are also known to age at 600°C, as has been described above, and in fact the formation of the rhombohedral phase causes a vast reduction in the ionic conductivity of the system.[71–73,77] Fung *et al.*[73] suggested that the addition of small amounts of ZrO_2 or ThO_2 to stabilise the Bi_2O_3–Y_2O_3 could be added (at quantities less than 5 mol%). Huang *et al.*[76] suggested that the addition of CeO_2 also suppresses the aging of Bi_2O_3–Y_2O_3.

Fully stabilised zirconia (FSZ) has also been added to fcc yttria stabilised bismuth oxide, to form a composite material, added to alleviate some of the problems described above, and to increase the mechanical integrity of the material.[78–82] The effect of zirconia additions on the oxygen ion conductivity is shown in Fig. 11.

3.3 Bi_2O_3–Er_2O_3

As can be seen from Fig. 12, the minimum value of x required to stabilise the fcc structure in $(Bi_2O_3)_{1-x}$ $(M_2O_3)_x$ versus the ionic radii of the Ln^{3+} ion, is quite marked. There appear to be two opposing tendencies; firstly, the ionic conductivity increases with increasing ionic radii, and secondly, the value for x_{min} increases with increasing radii. However, a high value for x_{min} produces a low ionic conductivity. Hence, as is shown in Fig. 13, the lowest value for x_{min} is for Er_2O_3 stabilised Bi_2O_3, which has been shown to have the highest oxygen ion conductivity,[83] as described in Fig. 12. Verkerk *et al.*[84] and Keizer *et al.*[85] examined the oxygen ion conductivity of $(Bi_2O_3)_{1-x}(Er_2O_3)_x$, and showed that the fcc structure was stable between 17.5 and 45·5 mol% Er_2O_3. Below and above these values, the sample existed as a multiphase material. The conductivity of the samples

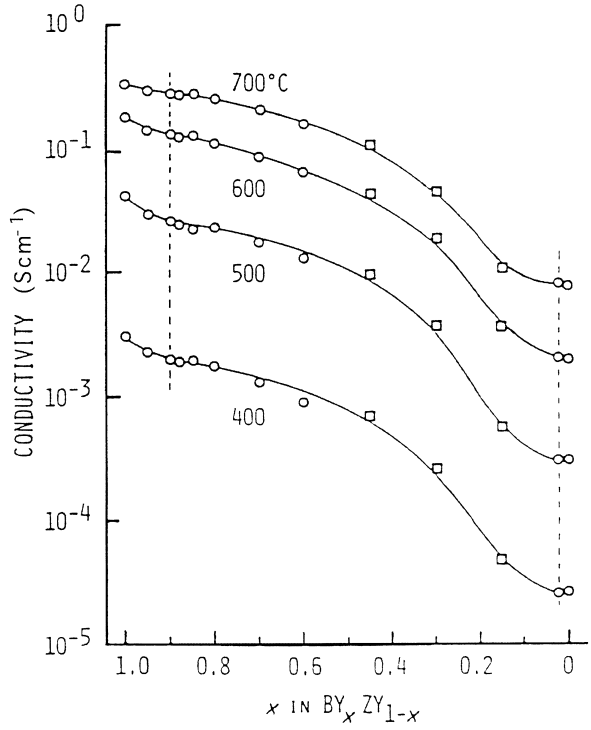

Fig. 11. Composition dependence of the conductivity in BY_xZY_{1x} measured for (open circles) normal sintered, and (open squares) hot-pressed specimens; dashed lines show solubility limits (Ref. 82).

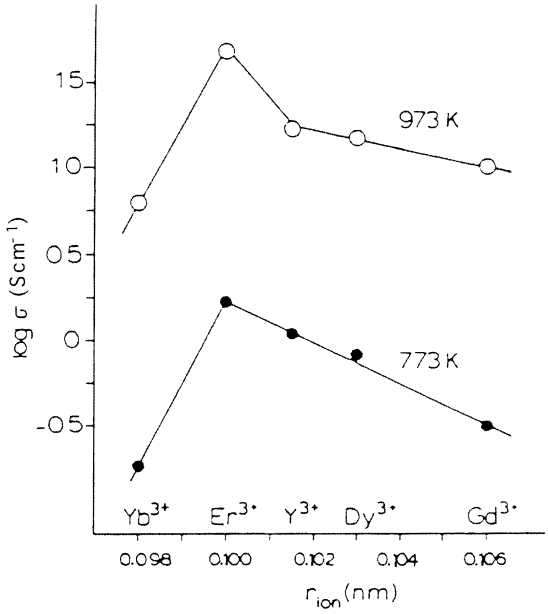

Fig. 12. The conductivity of $(Bi_2O_3)_{1x}(Ln_2O_3)_x$ for $x = X_{min}$ versus the ionic radius of the Ln^{3+} ion at 737 K (filled circles) and 973 K (open circles) (Ref. 25).

decreased with increasing Er_2O_3 content, as shown in Fig. 14. The existence of a fcc structure for $3Bi_2O_3{\cdot}Er_2O_3$ observed by Datta and Meehan[48] had, therefore, been confirmed by Verkerk *et al.*[84] However, the authors admitted that the existence of the fcc phase for $Bi_2O_3{\cdot}Er_2O_3$, as suggested by Nasonova *et al.*[86] was not proven. The authors

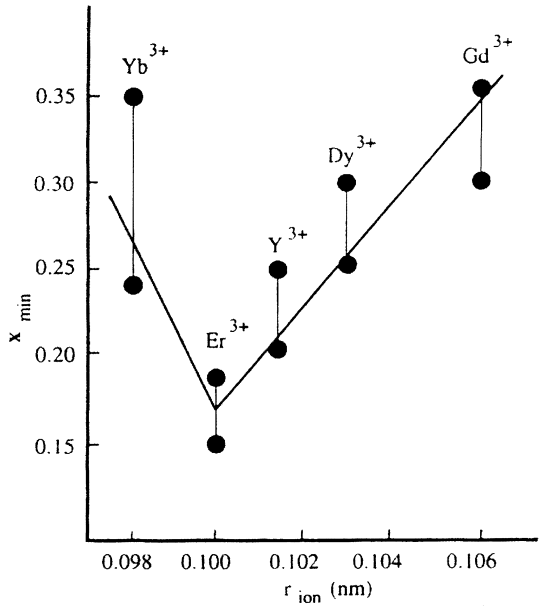

Fig. 13. X_{min} as a function of ionic radius (r_{ion}) of the dopant ion (Ref. 83).

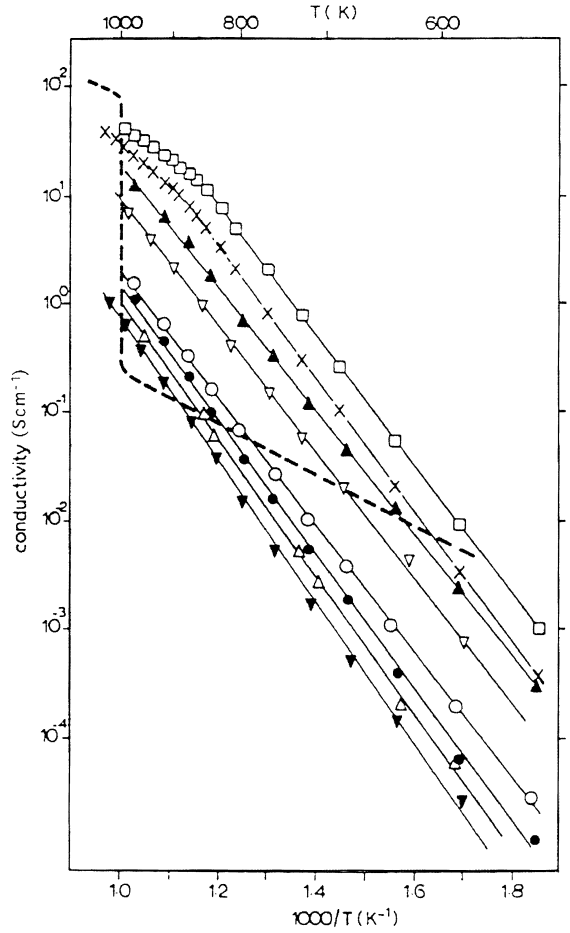

Fig. 14. Conductivity of $(Bi_2O_3)_{1-x}(Er_2O_3)_x$ in air; (□) $x=0{\cdot}2$, (X) $x=0{\cdot}25$, (▲) $x=0{\cdot}3$, (▽) $x=0{\cdot}35$, (○) $x=0{\cdot}4$, (●) $x=0{\cdot}455$, (△) $x=0{\cdot}5$, (▼) $x=0{\cdot}6$; the broken line represents the conductivity of pure Bi_2O_3 (Ref. 84).

also showed that $(Bi_2O_3)_{0{\cdot}8}(Er_2O_3)_{0{\cdot}2}$ had an ionic conductivity of 0·023 Scm^{-1} at 773 K, and 0·37 Scm^{-1} at 973 K, with an ionic transference number equal to unity. Jurado *et al.*[69] also investigated the dc electrical properties of $(Bi_2O_3)_{1-x}(Er_2O_3)_x$ and showed that one of the highest conductivities was for $(Bi_2O_3)_{0{\cdot}8}(Er_2O_3)_{0{\cdot}2}$. Later work by Bouwmeester *et al.*,[87] using oxygen permeability experiments, in conjunction with EMF measurements, confirmed that $(Bi_2O_3)_{1-x}(Er_2O_3)_x$ remained a solid electrolyte, under the conditions prevalent in their experimental work, with an ionic transference number close to unity.

Work by Verkerk *et al.*[88] showed that the electrode conductivity of Pt on a Bi_2O_3–Er_2O_3 electrolyte, was very much higher than for zirconia based electrolytes, and the diffusion of atomic oxygen on the oxide surface was the rate-determining step. Nagamoto and Inoue[89] later looked at Pt, Ag and $La_{1-x}Sr_xCoO_3$ electrodes on $(Bi_2O_3)_{1-x}(Er_2O_3)_x$, using current interruption techniques. The electrode resistance of the noble metals was approximately proportional to $PO_2^{-1/2}$, suggesting that the rate determining step was a diffusion process of the adsorbed oxygen, while the oxide electrodes varied from $PO_2^{-1/4}$ to $PO_2^{-1/2}$, indicating that both charge transfer and diffusion processes are rate determining.

Verkerk and Burggraaf[25] showed that the conductivity of $(Bi_2O_3)_{0{\cdot}8}(Er_2O_3)_{0{\cdot}2}$, in the temperature range 300–1100 K, displayed a bend in the Arrhenius behaviour. The activation energy was found to change from 115 to 62 kJ mol^{-1}. Neutron diffraction was then performed on the system, and the authors described that at low temperatures, short-range ordering in the oxygen lattice was apparent, while at higher temperatures the short-range ordering diminishes. This brings about an increase in the lattice constant and a subsequent decrease in the activation energy. Verkerk *et al.*,[90] using neutron diffraction, concluded that $(Bi_2O_3)_{1-x}(Er_2O_3)_x$ showed no long range ordering of the vacancies between 300 and 1100 K. At temperatures above 870 K, the lattice disorders and all the oxygen ions take part in the conduction process, while below 870 K, the activation energy of the conductivity is determined by the concentration of (Bi_3, Er)-tetrahedra.

Vinke *et al.*[91] investigated the oxygen pumping characteristics of $(Bi_2O_3)_{1-x}(Er_2O_3)_x$ using Au and Pt electrodes, and found that the material had very good pumping characteristics. Vinke *et al.*[92] investigated the electrode resistances of solid solutions of $(Bi_2O_3)_{0{\cdot}75}(Er_2O_3)_{0{\cdot}25}$ with sputtered and co-pressed gold electrodes. The results showed that the electrode configuration had only a minor role in the electrode resistance. The authors also found that the electrode reaction was not limited to the

triple phase boundary, instead that the electrolyte surface is very active; the electrode was postulated as only acting as a current collector. Vinke *et al.*[93] also showed a similar behaviour when sputtered Pt electrodes were used.

In a similar fashion to Y_2O_3-doped Bi_2O_3, the cubic phase of Er_2O_3-doped Bi_2O_3 also transforms into a hexagonal phase during annealing.[94] Later work by Kruidhof *et al.*[95] showed that the cubic solid solution of $(Bi_2O_3)_{1-x}(Er_2O_3)_x$ is metastable below 740°C, when $x < 0{\cdot}275$; the sample was found to gradually transform to the hexagonal phase during long term annealing at 650°C.

Battle *et al.*[44,96,97] using neutron scattering techniques, showed that the disorder described above for yttria-doped Bi_2O_3, can be used for $(Bi_2O_3)_{1-x}(Er_2O_3)_x$ systems, and explained that the conductivities of the 2 materials should be very similar. This is approximately found to be the case in the literature, and any large differences, the authors suggested, was due to preparation technique and powder source.

In trying to derive a model for the system $(Bi_2O_3)_{1-x}(Ln_2O_3)_x$, Verkerk *et al.*[90] proposed that an ordered unit is possible, and used the system $(Bi_2O_3)_{1-x}(Er_2O_3)_x$ as an example. The authors suggested that in a highly defective structure a completely random arrangement of vacancies is unfavourable and is only possible in very small domains, as suggested by Barker *et al.*[98] A model for the short range-ordered microdomains was given, and is shown in Fig. 15. Every tetrahedron consists of three Bi^{3+}-ions and one Ln^{3+}-ion, and was denoted as a (Bi_3-Ln) tetrahedron. The figure shows the oxygen ions of a (001) plane at $Z = 3/4$. The cations above and below this plane are also indicated. The cations are displaced in the direction of the lanthanide ions (as given by the Willis-type model, described above). This model fits well with the results observed for the knee in the Arrhenius plot of the Er_2O_3, Y_2O_3, Gd_2O_3 and Dy_2O_3-doped systems, which was reported as a change in the defect structure. However, as is seen in the model, there are 2 different O–O distances, one at 0·268 nm and one at 0·290 nm; the activation energy is determined by the strength of the Ln–O bond and the energy necessary for oxygen ions to migrate through the tetrahedral planes.

3.4 Bi_2O_3–La_2O_3

The cationic radii for La^{3+} is 1·18 Å, and as such $(Bi_2O_3)_{1-x}(La_2O_3)_x$ based solid solutions were found by Takahashi *et al.*[38] to correspond to a rhombohedral-type structure, rather than the fcc structure found in $(Bi_2O_3)_{1-x}(Er_2O_3)_x$, for example. Cahen *et al.*,[99] and the earlier work of Gattow and Schroder,[6] Levin and Roth[1] and Datta and

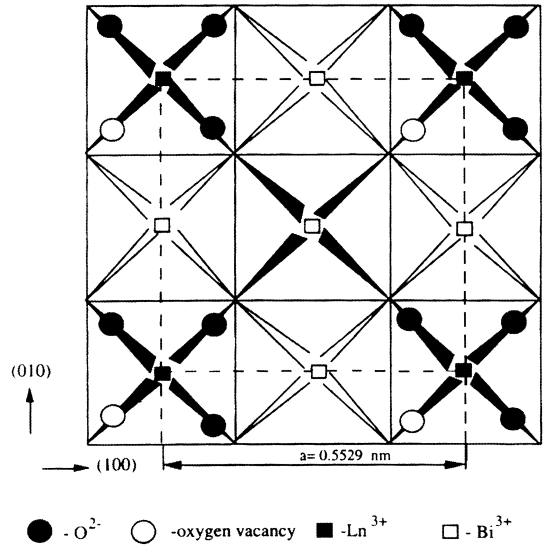

Fig. 15. A model of the ordered unit for $(Bi_2O_3)_{0.75}(Ln_2O_3)_{0.25}$. (□) = Bi^{3+} ion, (■) = Ln^{3+} ion, (●) = O^{2-} ion, (○) = O^{2-} vacancy; a = unit cell dimension (= 5·529 Å) (Ref. 90).

Meehan[48] could not find any fcc-stabilisation in $(Bi_2O_3)_{1-x}(La_2O_3)_x$. Takahashi *et al.*[38] showed that the ionic transport number was approximately 0·9, in the temperature range 550–750°C. Iwahara *et al.*[46] measured the ratios of the EMF of the concentration cell O_2 (0·21 atm), $Ag|(Bi_2O_3)_{1-x}(La_2O_3)_x|Ag$, O_2(1 atm), and showed the following results, as given in Table 4.

The oxygen ion conductivity values were plotted as a function of temperature for the cells, and are shown in Fig. 16 (which includes a number of other samples, including Nd_2O_3, and Er_2O_3-doped Bi_2O_3; the samples are also compared to fully stabilised zirconia). What the authors suggested was that rhombohedral $(Bi_2O_3)_{1-x}(La_2O_3)_x$ has one of the highest ionic conductivities of the bismuth oxide based systems. At high temperature, the material has a higher ionic conductivity than erbia-doped bismuth oxide, particularly in respect to 15 mol% La_2O_3-doped Bi_2O_3. The highest conductivity in this material was also found at the lower limit of La_2O_3 content, as shown in Fig. 12.

Mercurio *et al.*[100] examined the Bi_2O_3–Ln_2O_3–TeO_2 (Ln = La, Sm, Gd, and Er) from a conductivity and phase composition context. The authors showed, using powder X-ray diffraction, the presence of 5 non-stoichiometric phases, as well as 2 low temperature phases; $Bi_{10}Te_2O_{19}$ and $Bi_{16}Te_5O_{34}$. The composition domains are shown in Fig. 17, and show the 5 phases labelled:

(i) *Q*-phase; a tetragonal phase, isostructural with Bi_2O_3;
(ii) 2 fcc fluorite related solid solutions (*F* and *F'*);
(iii) An ε phase, isostructural with the rhombohedral phase;

Table 4. EMF values for doped bismuth oxide

Sample	*E/E₀*			
	500°C	*600°C*	*700°C*	*800°C*
$(Bi_2O_3)_{0.8}(La_2O_3)_{0.2}$	0·96	0·95	0·94	–

(iv) A solid solution labelled *R*, whose rhombohedral cell corresponds to a slight distortion of the fcc fluorite cell ($a = 5{\cdot}5689$Å, $\alpha = 92{\cdot}35°$).

The authors also suggested that the more highly distorted phases, the *F*, *F′* and *ε* had a higher ionic conductivity than the less disordered *Q* and *R* phases. In fact it was shown that the *R*-type $(Bi_2O_3)_{0.90}(La_2O_3)_{0.06}(TeO_2)_{0.04}$ had a higher ionic conductivity, of 5×10^{-3} S cm^{-1}, than $(Bi_2O_3)_{0.8}(La_2O_3)_{0.2}$ at 350°C.

Mercurio *et al.*[101] have also solved the structure of the *ε*-phase for the composition $Bi_{0.7}La_{0.3}O_{1.5}$, using X-ray and neutron diffraction techniques, and the schematic of the cell is shown in Fig. 18; the 2 possible pathways for the oxide ions are also given. The major drawback of the $(Bi_2O_3)_{1-x}(La_2O_3)_{x-y}(TeO_2)_y$ solid solution is that there is a strong possibility that the Te^{4+} ion may reduce even at relatively high oxygen partial pressures, causing a degradation in the electrolytic properties of the material.

3.5 Bi_2O_3–Dy_2O_3

The occurrence of the fcc phase in $(Bi_2O_3)_{1-x}(Dy_2O_3)_x$ was first reported by Datta and Meehan[48] for the phase $3Bi_2O_3{\cdot}Dy_2O_3$, and for the phase $Bi_2O_3{\cdot}Dy_2O_3$ by Nasanova *et al.*[86]

Verkerk and Burggraaf[102] examined the phase diagram and oxygen ion conductivity of the $(Bi_2O_3)_{1-x}(Dy_2O_3)_x$ system. The sample containing 5 mol% Dy_2O_3 has a tetragonal structure. The samples containing between 10 and 25 mol% Dy_2O_3 were rhombohedral at room temperature, although a metastable high temperature fcc phase could be formed at room temperature by quenching. Samples containing between 28·5 to 50 mol% Dy_2O_3 had the equilibrium fcc structure at room temperature. The results of Verkerk and Burggraaf[102] did not, therefore, agree with the results of Datta and Meehan;[48] it is possible that Datta and Meehan had measured the non-equilibrium fcc structure.

Verkerk and Burggraaf[102] also investigated the ionic conductivity of the material, and suggested that all the cations in $(Bi_2O_3)_{1-x}(Dy_2O_3)_x$ occupy their normal sites in the fluorite structure in a unit cell; $Bi_{4(1-x)}Dy_{4x}O_{6\square 2}$, where $\square$ is an oxygen vacancy. Figure 19 shows the ionic conductivity of $(Bi_2O_3)_{1-x}(Dy_2O_3)_x$ from $x = 0{\cdot}25$ to 0·6. It is apparent that the highest conductivity, for a stable fcc structure, was reported for the sample $x = 0{\cdot}285$, with a value of $7{\cdot}1\times10^{-3}$ Scm^{-1} at 500°C, and 0·14 Scm^{-1} at 700°C.

The ionic transference number was measured using an oxygen concentration cell on samples containing between 25 and 60 mol% Dy_2O_3. Only

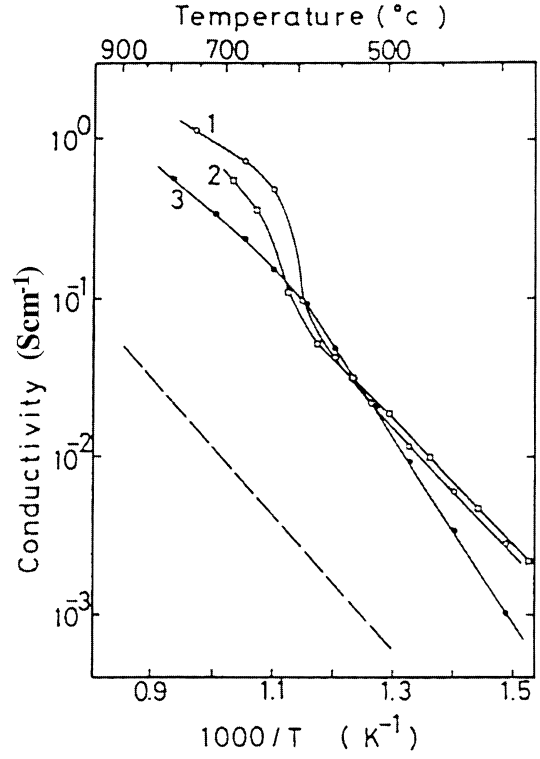

Fig. 16. Arrhenius plots of conductivity of sintered oxides of the system $(Bi_2O_3)_{1-x}(Ln_2O_3)_x$; (1) $x = 0{\cdot}1$, Ln = Nd; (2) $x = 0{\cdot}15$, Ln = La; (3) $x = 0{\cdot}25$, Ln = Er. The broken line represents the conductivity of $(ZrO_2)_{0.9}(Y_2O_3)_{0.1}$ (Ref. 46).

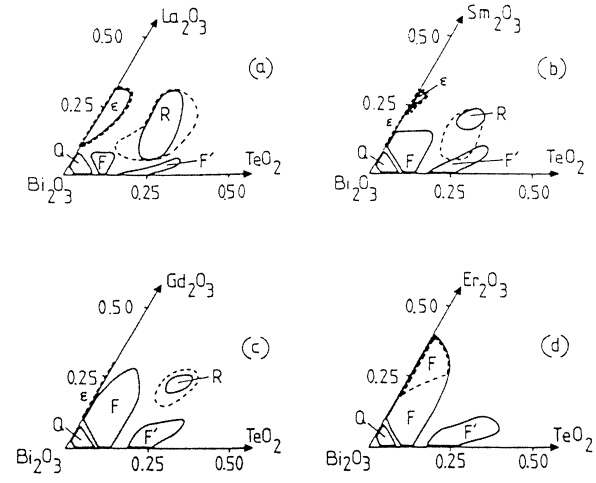

Fig. 17. Composition domains at 800°C and at room temperature for the phases isolated in the Bi_2O_3-rich region of the pseudo-ternary Bi_2O_3–Ln_2O_3–TeO_2 systems; (a) Ln = La; (b) Ln = Sm; (c) Ln = Gd; (d) Ln = Er. (– – –) slow cooling to room temperature, (—) quenching from 800°C (Ref. 100).

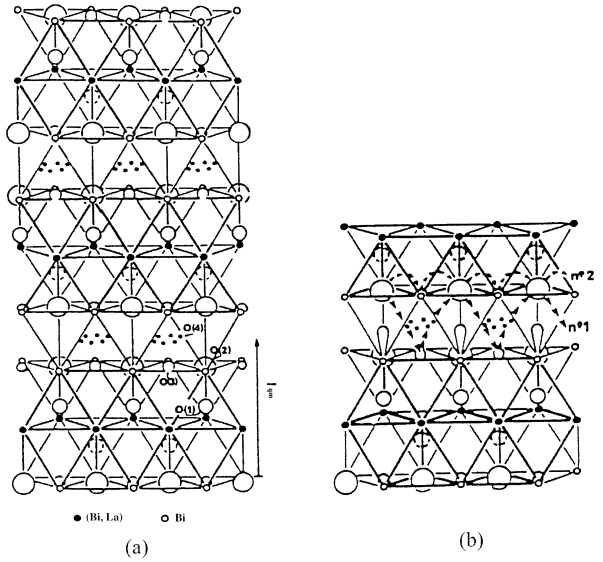

Fig. 18. (a) Schematic view of the $Bi_{0.7}La_{0.3}O_{1.5}$ crystal structure; (b) possible diffusion pathways for the oxide ions in the $Bi_{0.7}La_{0.3}O_{1.5}$ phase (Refs. 100, 101).

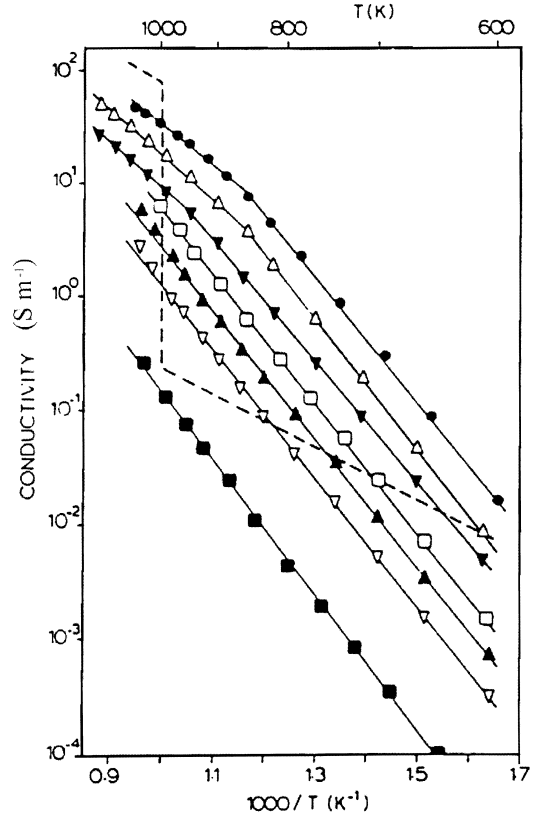

Fig. 19. Conductivity of $(Bi_2O_3)_{1-x}(Dy_2O_3)_x$ in air; (●) $x=0{\cdot}25$, (△) $x=0.285$, (▼) $x=0{\cdot}35$, (□) $x=0{\cdot}4$, (▲) $x=0{\cdot}45$, (▽) $x=0{\cdot}5$, (■) $x=0{\cdot}6$; the broken line represents the conductivity of pure Bi_2O_3 (Ref. 25).

at samples containing 50 mol% Dy_2O_3 or greater was there any appreciable electronic component. It was postulated that the high electronic component in the 60 mol% Dy_2O_3 was due to a multi-phase sample, containing a Dy_2O_3-rich phase, which is known to be an electronic conductor.[103] Iwahara *et al.*[46] and Verkerk and Burggraaf[25] who also examined $(Bi_2O_3)_{1-x}(Dy_2O_3)_x$ as part of work on the sequence $(Bi_2O_3)_{1-x}(Ln_2O_3)_x$, found similar results to that of the work of Verkerk and Burggraaf,[102] and showed good ionic conductivity in the samples. However, both authors agreed that the best conductivity was found for the samples containing Er or Tm as the dopant.

Watanabe[104] investigated the polymorphism of $Bi_{1-x}Ln_xO_{1.5}$ (where Ln = Sm, Eu, Gd, Tb and Dy, and $x=0{\cdot}38$, $0{\cdot}375$, $0{\cdot}275$–$0{\cdot}4$, $0{\cdot}275$–$0{\cdot}35$, and $0{\cdot}3$–$0{\cdot}35$, respectively). Thus, the author examined $(Bi_2O_3)_{1-x}(Dy_2O_3)_x$ from 0·3 to 0·35, and showed that the material contained a novel phase, C-phase. The C-phase was only apparent after a repetitive heat treatment cycle, in fact for $Bi_{0.675}Dy_{0.325}O_{1.5}$, the sample only formed the C-phase after 4 heat cycles at approximately 815°C/417 h. The C-phase was a low temperature bcc phase crystallised with the space group $I2_13$, where $a=10{\cdot}987$ Å and $Z=32$.[105] The C-phase was also found to have a very low ionic conductivity, of approximately $10^{-3{\cdot}9}$ S cm^{-1} at 700°C. In conclusion, Watanabe[104] suggested that δ-Bi_2O_3 stabilised with Ln_2O_3 (Ln = Sm, Eu, Gd, Tb, and Dy) is always metastable at low temperatures, and that the true stable low temperature phase has a C-type rare-earth oxide related structure, and transforms, on heating, to the δ-phase at approximately 900°C.

3.6 Bi_2O_3–Gd_2O_3

As shown in Fig. 13, earlier, the maximum amount of Gd^{3+} required to stabilise Bi_2O_3 is approximately 35 mol%, which would suggest that, due to the relatively high percentage, that the Bi_2O_3–Gd_2O_3 system would have one of the lowest ionic conductivities of the M_2O_3 doped systems; this is confirmed in Fig. 12.

Datta and Meehan[48] investigated the equilibrium relationships in the system Bi_2O_3–Gd_2O_3, and observed the formation of the fcc phase over a wide range of compositions and temperature. They also noted that when the unit lattice parameter of the fcc phase was plotted against mol% Gd_2O_3, a discontinuity occurred. This was explained as being due to the formation of Bi_3GdO_6, with cell dimensions of 5·525 Å. Takahashi *et al.*[64] showed that the fcc structure observed by Datta and Meehan[48] was unstable at low temperatures, and reverted to a tetragonal structure between 5 and 10 mol% Gd_2O_3, and to a rhombohedral structure between 10 and 30 mol% Gd_2O_3. The authors also suggested that both the fcc and rhombohedral phases were good oxide ion conductors. Koto *et al.*[106] used single crystal X-ray diffraction to investigate the structure of $(Bi_2O_3)_{1-x}(Gd_2O_3)_x$. The authors showed that the displacement of oxide ions from

the normal tetrahedral sites decreases with increasing x, and was found to be zero at $x = 0{\cdot}32$. They also found that the fcc phase could be quenched in when $x = 0{\cdot}1$–$0{\cdot}3$, although the phase was not fcc for $x = 0{\cdot}02$–$0{\cdot}05$. Watanabe,[104] however, observed the C-type structure in Gd_2O_3-doped Bi_2O_3 between dopant concentrations of 27·5– 40 mol%. As was the case for Dy_2O_3 doped Bi_2O_3, described above, the bcc C-phase was also suggested as being the stable phase in this system, and that the fcc δ-phase is only metastable. The conductivity of the C-phase was also shown to be lower than that of the metastable fcc phase.

Takahashi and Iwahara[50] showed that the conductivity curves of $(Bi_2O_3)_{1-x}(GdO_{1{\cdot}5})_x$ at $x < 0{\cdot}35$ showed an abrupt increase in the conductivity due to the phase transformation from tetragonal (or rhombohedral) to cubic. At $x > 0{\cdot}35$, a single linear correlation was observed. The conductivity of these samples was examined in the range 1–10^{-5} atm oxygen partial pressure, and was observed to be purely ionic in nature.

3.7 Other Bi_2O_3–Ln_2O_3 (Ln = Sm, Eu, Tb, Ho, Tm, Yb, Lu)

A variety of these oxide dopants have been claimed to be able to stabilise the fcc δ-Bi_2O_3 to room temperature. The work has been summarised in Table 5 and as is observed by the table, there is much confusion about the ability to stabilise the fcc structure, or not.

Cahen *et al.*[99] discussed the electrical conductivity of δ-Bi_2O_3 stabilised by rare-earth oxides. The authors showed that all the rare earths, from Tb to Lu (atomic numbers from 65 to 71), proved to stabilise the fcc structure at 25 mol% dopant, as reported by Datta and Meehan earlier.[48] However, Cahen *et al.*[99] showed that Gd^{3+} could not stabilise the fcc structure, whereas Datta and Meehan found a stable fcc structure. Verkerk and Burggraaf[83] investigated the effect of ionic radius on the electrical conductivity of $(Bi_2O_3)_{1-x}(Ln_2O_3)_x$ for x_{min} (as described above). They showed that the ionic conductivity increases with increasing ionic radius, and that the value of x_{min} increases with increasing ionic radius; a high x_{min} results in a low ionic conductivity. Thus, the best value was found from $Ln = Er^{3+}$, as described in Figs 12 and 13. Watanabe,[104] however, found that the C-phase was present in $Bi_{1-x}Ln_xO_{1{\cdot}5}$ (Ln = Sm, Eu, Gd, Tb, and Dy), which had the bcc structure and was formed when the sample had been annealed at 800°C. The ionic conductivity of the C-phase was lower than that of the fcc phase. Watanabe[108] also observed a hexagonal structure in the $(Bi_2O_3)_{1-x}(Ho_2O_3)_x$ system. The phase formed a solid solution $Bi_{2-2x}Ho_{2x}O_3$ ($x = 0{\cdot}205$–$0{\cdot}245$ at 650°C), having a $Bi_{0{\cdot}765}Sr_{0{\cdot}235}O_{1{\cdot}383}$-type layered structure with hexagonal symmetry. This phase was found to transform reversibly into the high temperature δ-Bi_2O_3 between 715 and 735°C depending on the value of x. The author also found that the hexagonal structure had good ionic conductivity.

Esaka and Iwahara[107], following on from the work of Datta and Meehan[48] and Cahen *et al.*[99] investigated the properties of $Tb_2O_{3{\cdot}5}$·Bi_2O_3 systems. The authors showed that oxide ion conduction was observed in the low temperature β-rhombohedral phase, and the high temperature fcc phase when less than 20 mol% $Tb_2O_{3{\cdot}5}$ was used. At dopant concentrations greater than 30 mol%, the authors claimed that the fcc structure could be stabilised to lower temperatures; the authors also showed that electronic conduction (due to electron holes) appeared in those samples containing between 30 and 50 mol% $Tb_2O_{3{\cdot}5}$.

In summary, Table 6 summarises typical conductivity values at a number of temperatures, and structures, of some $(Bi_2O_3)_{1-x}(Ln_2O_3)_x$ systems.

3.8 $(Bi_2O_3)_{1-x}(M_2O_5)_x$ (M = V, Nb, P, Ta)

Takahashi *et al.*[109] examined the electrical conductivity, ionic transference number, and phase equilibrium of Bi_2O_3–M_2O_5 (M = V, Nb, and Ta). Table 7 summarises the phase equilibrium the authors observed for a number of annealed and quenched samples.

Table 5. Literature describing no fcc and fcc stabilisation of bismuth oxide

Ln	*References showing no fcc stabilisation*	*References showing fcc stabilisation*
Sm	1,5 = 6,48,104	–
Eu	48,104	–
Tb	104,107	48,107
Ho	108	48
Tm	–	99
Yb	48	99
Lu	1,48	99

Table 6. Conductivity values at various temperature, observed fro structures of $(Bi_2O_3)_{1-x}(Ln_2O_3)_x$ systems

Composition	*Temperature (°C)*	*Structure*	*Conductivity (S cm^{-1})*	*Reference*
Bi_2O_3	800	fcc	2·3	1
$Bi_{0{\cdot}75}Y_{0{\cdot}25}O_{1{\cdot}5}$	600	fcc	$4{\cdot}38\times10^{-2}$	55
$Bi_{0{\cdot}65}Y_{0{\cdot}20}O_{1{\cdot}5}$	600	fcc	$2{\cdot}5\times10^{-2}$	55
$Bi_{0{\cdot}65}Gd_{0{\cdot}35}O_{1{\cdot}5}$	650	fcc	$5{\cdot}6\times10^{-2}$	51
$Bi_{0{\cdot}8}Tb_{0{\cdot}2}O_{1{\cdot}5}$	650	fcc	0·28	107
$Bi_{0{\cdot}71}5Dy_{0{\cdot}285}O_{1{\cdot}5}$	700	fcc	0·14	102
$Bi_{0{\cdot}75}Ho_{0{\cdot}25}O_{1{\cdot}5}$	650	fcc	0·17	99
$Bi_{0{\cdot}80}Er_{0{\cdot}20}O_{1{\cdot}5}$	600	fcc	0·23	69
$Bi_{0{\cdot}80}Er_{0{\cdot}20}O_{1{\cdot}5}$	700	fcc	0·37	75
$Bi_{0{\cdot}75}Tm_{0{\cdot}25}O_{1{\cdot}5}$	650	fcc	$8{\cdot}0\times10^{-2}$	99
$Bi_{0{\cdot}65}Yb_{0{\cdot}35}O_{1{\cdot}5}$	700	fcc	$6{\cdot}3\times10^{-2}$	51
$Bi_{0{\cdot}7}Gd_{0{\cdot}3}O_{1{\cdot}5}$	700	fcc	$1{\cdot}0\times10^{-2}$	25
$Bi_{0{\cdot}75}Lu_{0{\cdot}25}O_{1{\cdot}5}$	650	fcc	$3{\cdot}7\times10^{-2}$	99

Table 7. Phase equilibria observed for various of annealed and quenched samples of doped bismuth oxide systems

M	*Mol% M_2O_5*	*Phases observed*	
		Annealed sample	*Quenched sample*
V	5–9	fcc + bcc	fcc
V	10–20	fcc + ?	?
Nb	5–12·5	fcc + mon	fcc
Nb	15–25	fcc	fcc
Nb	30	fcc + tetragonal	fcc + tetragonal
Ta	3–7·5	tetragonal	fcc
Ta	10–16	fcc + tetragonal	fcc
Ta	18–25	fcc	fcc
Ta	33	fcc + ?	fcc + ?

Table 8. Summary of the findings of the Bi_2O_3–V_2O_5 systems from a number of authors

Composition (mol% V_2O_5)	*Formula*	*Reference*
12·5	Bi_7VO_3	111
22·222	$Bi_{14}V_4O_{31}$	112
14·286	$Bi_{12}V_2O_{23}$	113
20	$Bi_8V_2O_{17}$	113
12·5	Bi_7VO_{13}	114
16·667	Bi_5VO_{10}	114
22·222	$Bi_{14}V_4O_{31}$	114
14·286	$Bi_{12}V_2O_{23}$	115, 116
20	$Bi_8V_2O_{17}$	115, 116
22·222	$Bi_{14}V_4O_{31}$	115, 116
14·286	$Bi_{12}V_2O_{23}$	117
14·815	$Bi_{23}V_4O_{44·5}$	118

The fcc phase was analogous to the high temperature fcc δ-Bi_2O_3 phase observed in the annealed samples of Bi_2O_3–Nb_2O_5 (15–25 mol%), and in Bi_2O_3–Ta_2O_5 (18–25 mol%). The authors observed no single phase in Bi_2O_3–V_2O_5, suggesting that the fcc phase had a very narrow composition range, or that some metastable phases were mixed in. In fact, a number of investigators have reported intermediate phases present in the Bi_2O_3–V_2O_5, as well as the Bi_2O_3–P_2O_5, systems. Table 8 summarises the findings of the Bi_2O_3–V_2O_5 systems from a number of authors. Figure 20 shows the revised phase equilibrium diagram for Bi_2O_3–Nb_2O_5, taken from Powers who suggested that the pure fcc structure was not observed at high concentrations of Nb_2O_5. Levin and Roth[1] suggested that a fcc phase, analogous to the Bi_2O_3–Nb_2O_5 system, could exist in Bi_2O_3–Nb_2O_5, although the authors did not put forward any phase equilibrium diagrams.

Watanabe[118] observed that the phases $Bi_{23}V_4O_{44·5}$ and $Bi_{23}P_4O_{44·5}$, had the triclinic structure based on the pseudo-fcc subcell. The author also observed very high ionic conductivity, particularly for $Bi_{23}P_4O_{44·5}$; approximately 10^{-2} S cm^{-1} at 600°C. Takahashi *et al.*[109] also observed very high ionic conductivity in the samples, particularly those that contained the fcc phase, although the authors found that the maximum conductivity was found at the lower limit of the fcc solubility range (12·5 mol% for V_2O_5, 15 mol% for Nb_2O_5, and 18 mol% for Ta_5O_5), and decreased with increasing dopant concentration. However, Powers[110] suggested that the solid solutions containing 10–14 mol% Nb_2O_5 were only the fcc-phase, while those containing 15–21 mol% Nb_2O_5 consisted of 2 phases; the fcc δ-phase, and another phase similar to the fcc phase, labelled δ'. Watanabe,[60] however, reported that the fcc-phase could not be stabilised with Nb_2O_5, Ta_2O_5 or V_2O_5 as dopants in Bi_2O_3. In V_2O_5, a sillenite phase was recognised at approximately 6·5 mol% V_2O_5; above this composition a two phase region containing and

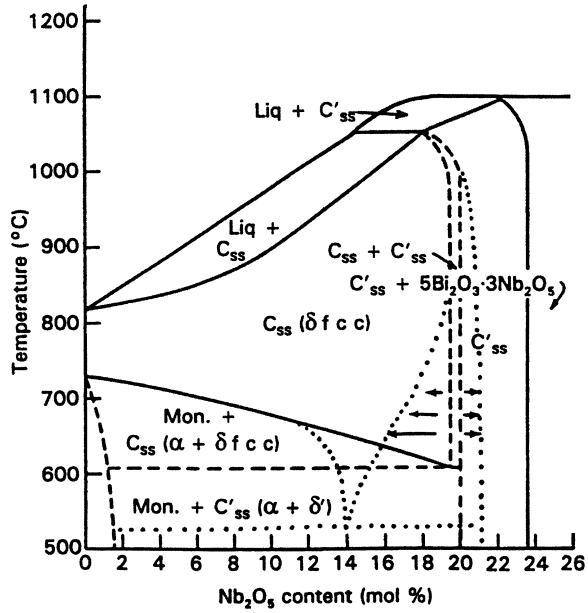

Fig. 20. Phase equilibrium diagram for the Bi_2O_3–Nb_2O_5 system (Ref. 110).

an unknown phase was observed. The high temperature δ-Bi_2O_3 could be quenched to room temperature in the system Bi_2O_3–Nb_2O_5, however it decomposed on annealing to a low temperature stable modification α-Bi_2O_3. In the system Bi_2O_3–Ta_2O_5, several phases were formed depending on the composition. At approximately 2 mol% Ta_2O_5, a β-modification was formed and the fcc phase was observed at approximately 8 mol% Ta_2O_5. Both phases, however, decomposed when annealed.

In the $(Bi_2O_3)_{1-x}(M_2O_5)_x$ system, Takahashi *et al.*[109] observed that the highest ionic conductivity was for the system $(Bi_2O_3)_{0·85}(Nb_2O_5)_{0·15}$, having an ionic conductivity of $1·9\times10^{-1}$ S cm^{-1} at 700°C, although the material was unstable in reducing environments. Powers,[110] however, found that the maximum conductivity was observed at 9 mol% Nb_2O_5, and showed that the ionic conductivity of

$(Bi_2O_3)_{0.85}(Nb_2O_5)_{0.15}$ was much lower than that observed by Takahashi *et al.*,[109] Meng *et al.*[74] ($1{\cdot}9\times10^{-1}$ S cm^{-1} at 700°C for $(Bi_2O_3)_{0.8}(Nb_2O_5)_{0.2}$), and Joshi *et al.*[56] (4×10^{-2} S cm^{-1} at 700°C for $(Bi_2O_3)_{0.85}(Nb_2O_5)_{0.15}$). Thus, there is still much controversy over the ionic conductivity of these phases, particularly at the higher temperatures. In fact Joshi *et al.*[56] did suggest that these systems were preferable for applications at temperatures lower than 650°C.

A detailed study of the Aurivillius-like phases of $Bi_2V_{n-1}BnO_{3n+3}$ (B = metal cation on the B-site, such as Ti^{4+}, Nb^{5+}, Ta^{5+}, etc.) and related structures, will be examined in the next section.

3.9 BIMEVOX and Aurivillius phases

Lu and Steele[119] investigated the ionic conductivity of the scheelite oxide $BiVO_4$ with and without 1 mol% CaO, and showed the material to be an oxygen ion conductor, with a relatively good ionic conductivity, particularly at lower temperatures, although *p*-type conductivity was suggested at high temperature. The initial work of Debreuille-Gresse[120] for the phase equilibrium of Bi_2O_3–V_2O_5 showed a scheelite phase, $BiVO_4$, which had been well characterised by a number of authors.[121–123] Ramadass *et al.*[124] reported that, depending on the stoichiometry of $BiVO_{4-x}$, it showed *p*-type or *n*-type mixed conductivity. Vinke *et al.*,[125] following on from the work of Boukamp *et al.*[126] and Burggraaf *et al.*[127] examined the electrical conductivity of $BiVO_4$, and observed that the total conductivity was approximately 1 order of magnitude lower than yttria stabilised zirconia, with an ionic transference number of 0·65 at 810 K and 0·25 at 940 K. They also showed, using Seebeck measurements that the material was an *n*-type mixed conductor.

Following from the work on $BiVO_4$, Abraham *et al.*[128] were possibly the first to thoroughly examine the phase $Bi_4V_2O_{11}$, and showed that the material consisted of Bi_2O_2 layers interleaved with V_2O_7 sheets, and has three reversible transitions at 720, 840 and 1150 K. These phase transitions were noted as being:

1. α to β at 720 K on heating;
2. β to γ at 840 K on heating;
3. γ to γ' at 1150 K on heating;
4. liquid at 1160 K.

α-$Bi_4V_2O_{11}$ was indexed to the face centred orthorhombic cell, with cell parameters $a = 0{\cdot}5533(1)$ nm, $b = 0{\cdot}5611(1)$ nm, and $c = 1{\cdot}5288$ nm. β-$Bi_4V_2O_{11}$ was indexed to a tetragonal cell, with parameters $a = b = 1{\cdot}1285(8)$ nm, and $c = 1{\cdot}542(1)$ nm at 775 K. γ-$Bi_4V_2O_{11}$ was found to be tetragonal, with cell parameters $a = 0{\cdot}3988(2)$ nm, and $c = 1{\cdot}542(1)$ nm at 885 K, with space group I4/mmm.[129]

On cooling, an intermediate phase was formed at 680 K, called $\alpha,'$. The ionic conductivity appeared to be very good for the high temperature modification, γ, with a transport number very close to unity.

$Bi_4V_2O_{11}$, belonging to the Aurivillius layered-perovskite family,[130] has $[Bi_2O_2]^{2+}$ layers alternating with $(VO_{3\cdot5}(V\ddot{o})_{0\cdot5})^{2-}$ oxygen deficient perovskite slabs. The oxygen vacancies are responsible for the high ionic conductivity observed in the material;[128] Fig. 21 shows the ideal structure of γ-$Bi_4V_2O_{11}$. Lee *et al.*[131] investigated the phase-equilibrium of the system Bi_2O_3–V_2O_5, and the results are shown in Fig. 22. The work was, in part, undertaken due to the confusion of the earlier work on the phase equilibrium.[114] The authors showed the existence of the phase $Bi_4V_2O_{11}$ and its polymorphic transitions at approximately 450 and 550°C, although they observed a slightly V_2O_5-deficient phase at most temperatures. The existence of the high temperature phase γ' was refuted, and the authors suggested that the transition is associated with the onset of melting at the solidus temperature.

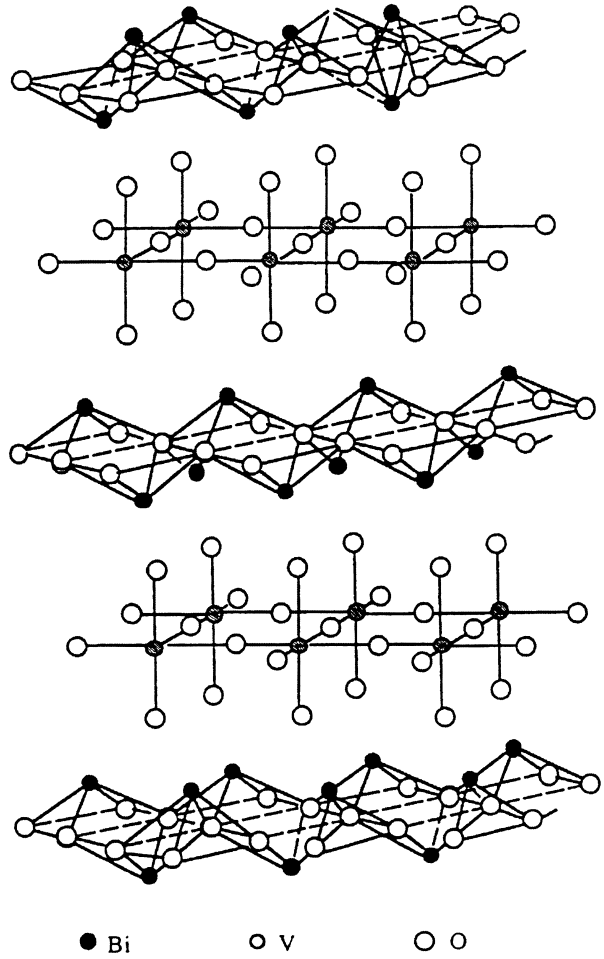

Fig. 21. The schematic representation of the ideal structure of γ-$Bi_4V_2O_{11}$ phase (Ref.150).

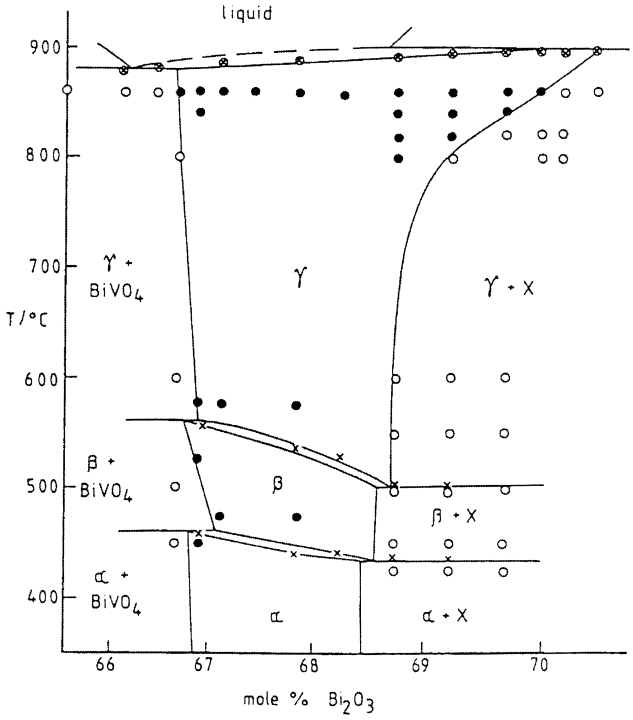

Fig. 22. Stoichiometry-stability of $Bi_4V_2O_{11}$ solid solutions: (⊗) melting temperatures of the pellets, (X) DTA transition temperatures on heating (●) single phase, and (○) multiphase samples, as shown by X-ray diffraction on quenched samples. The identity of *X* is unknown (Ref. 114).

As has been described above, the high temperature γ-$Bi_4V_2O_{11}$ has a high ionic conductivity due to the high disorder in the material, however at lower temperatures, the structure becomes ordered, the unit cell much larger, and the conductivity appreciably lower. Thus, Abraham *et al.*[129] considered the possibility of partial substitution of the vanadium by other metal ions such as Cu and Ni. The acronym BIMEVOX (BI = bismuth, ME = metal ion, V = vanadium, and OX = oxide) was given to this new family of materials. Abraham *et al.*[129] studied the BICUVOX series, using Cu as the substitute metal ion, $Bi_2V_{1-x}Cu_xO_{5.5-3x/2}$ from $x = 0$–0·12. From $x = 0$ to 0·07, the cell was found to be orthorhombic and isotypic with the α-$Bi_4V_2O_{11}$, however from $x = 0{\cdot}07$ to 0·12, the sample was observed as being tetragonal, and of the γ-$Bi_4V_2O_{11}$ type. The conductivity of $Bi_2V_{0.9}Cu_{0.1}O_{5.35}$, for example, was found to be 3×10^{-3} S cm^{-1} at 510 K. Iharada *et al.*[132] investigated the partial substitution of Cu and Ni for $Bi_4V_2O_{11}$, and showed high ionic conductivity and an ionic transport number close to unity, although they observed significant *n*-type behaviour at low oxygen partial pressures for both metal substitutions. Although the variation laws of conductivity versus oxygen partial pressure were not studied in detail, the authors suggested that the system was possibly in a transition between two regimes. Reiselhuber *et al.*[133] observed the effect of grain size and synthesis route on the ionic properties of BICUVOX, and showed a difference in the conductivity between large grains and small grains in the fired ceramic material. Anne *et al.*[134] and Pernot *et al.*[135] also studied the structure and conductivity of BICUVOX and BINIVOX materials, and showed that the high temperature phase could be stabilised to room temperature. Francklin *et al.*,[136] using EXAFS, studied $Bi_4V_2O_{11}$ and BICUVOX materials, and showed that the oxygen ion is the mobile species at moderate temperature, however they suggested that the migration process is not via simple vacancy hopping.

Sharma *et al.*[137] substituted up to 10 atm% of Li^+, Zn^{2+}, Al^{3+}, Ti^{4+} and Ge^{4+} for V in $Bi_4V_2O_{11}$, and the conductivities are summarised in Table 8. They observed that the best ionic conductor was for $Bi_4V_{1.8}Ti_{0.2}O_{10.9}$, and explained that the ionic potential of the substituting cation was more important than the oxygen vacancy concentration in determining the oxygen ion conductivity of the material. Goodenough *et al.*[138] showed that they could not substitute Mo^{6+} nor W^{6+} for V^{5+} in $Bi_4V_2O_{11}$, but could substitute Nb, over the compositional range of $x = 0$–1·0 in $Bi_4V_{2-x}Nb_xO_{11}$. Among the phases investigated by the authors, only $Bi_4V_{1.8}Ti_{0.2}O_{11-\delta}$, $Bi_4V_{1.8}Nb_{0.2}O_{11}$ and $Bi_{3.8}Pb_{0.2}V_{1.8}Nb_{0.2}O_{11-\delta}$ showed fast oxygen ion conduction comparable to that found with $Bi_4V_{1.8}Cu_{0.2}O_{11-\delta}$, discovered by Abraham *et al.*[129]. Vannier *et al.*,[139] however, showed that the phase $Bi_2V_{1-x}Mo_xO_{(11+x)/2}$ could be formed up to $x = 0{\cdot}225$. with high oxide ion conductivity. Vannier *et al.*[140] also studied the phases $Bi_2V_{1-x}Pb_xO_{(11-3x)/2}$, with x up to 0·1, $Bi_{2-y}Pb_yVO_{(11-y)/2}$, with y up to 0·2, and $Bi_{1.9}Pb_{0.1+x}V_{1-}xO_{(10.9-3x)/2}$, with x up to 0·12, and showed that the material was isostructural with $Bi_4V_{1.8}Cu_{0.2}O_{11-\delta}$, with good ionic conductivity at high temperature, however greatly reduced conductivity at low temperature. The oxide ion transport number was found to be between 0·9 and 0·95 between 720 and 1120 K; slightly lower than those observed for the Cu substituted materials.

Vannier *et al.*[141] studied the double substitution either on the Bi site, or on the V-site using a variety of double dopants. There was no improvement of the ionic conductivity over that of the singly doped BICUVOX system.

Over the last few years, a number of authors have investigated the ionic conductivity of a range of BIMEVOX systems, including: Cr,[142,143] Fe,[142] Co,[143–146] Zn,[147,142] Ni,[147] La,[148] Y,[148], Mg,[148] B,[148] Sb,[149,142] Nb,[149,143] Ti,[143,150] W,[143,151] Ta,[143] Mo,[132] Zr,[150] Sn,[150] Pb,[150] and U.[152] The ionic conductivity of a range of these systems is summarised in Table 9.

Table 9. Ionic conductivities reported for BIMEVOX systems

Sample	*Temperature (K)*	*Ionic conductivity (S cm^{-1})*	*Reference*
$Bi_4V_{1.7}Sb_{0.3}O_{11}$	590	10^{-2}	149
$Bi_4V_{1.7}Nb^{0.3}O_{11}$	590	10^{-3}	149
$Bi_4V_{1.7}Ti_{0.3}O_{10.85}$	500	4×10^{-4}	150
$Bi_4V_{1.8}Pb_{0.2}O_{10.9}$	500	2.5×10^{-6}	150
$Bi_4V_{1.8}Zr_{0.2}O_{10.9}$	500	4.1×10^{-6}	150
$Bi_4V_{1.8}Sn_{0.2}O_{10.9}$	500	4.4×10^{-6}	150
$Bi_4V_{1.8}Ti_{0.2}O_{10.9}$	500	6.3×10^{-5}	150
$Bi_4V_{1.8}La^{0.2}O_{10.8}$	573	$1.4\times10^{-}$	148
$Bi_4V_{1.8}Zn_{0.2}O_{10.70}$	500	1.28×10^{-4}	147
$Bi_4V_{1.8}Ni_{0.2}O_{10.70}$	500	3.05×10^{-4}	147
$Bi_4V_{1.8}B_{0.2}O_{10.8}$	573	2.0×10^{-5}	148
$Bi_4V_{1.8}Y_{0.2}O_{10.8}$	573	1.0×10^{-4}	148
$Bi_4V_{1.8}Mg_{0.2}O_{10.7}$	573	1.1×10^{-3}	148

There is still much controversy as to the major factors that affect the ionic conductivity of the $Bi_4V_{2-x}M_xO_{11-x/2}$ system. It is not clear whether it is due to the oxygen vacancy concentration, or the nature of the substituent ions, or some other variable that is most effective in stabilising the highly conductive phase. Some systematic studies have been undertaken. Yan and Greenblatt[150] showed that the γ-phase can be stabilised by using Ti, Zr, Sn and Pb and at $x > 0.2$ in $Bi_4V_{2-x}M_xO_{11-x/2}$. In general the authors found that the conductivities, at 500 K, decreased in the order Ti > Sn > Zr > Pb, for a given γ-composition. Lazure *et al.*[143] undertook a similar study on a wide range of materials, and observed that the maximum conductivity values are obtained when x values are close to the lower limit of the solid solution with the γ-type structure. A number of phase equilibrium diagrams have been examined Bi_2O_3–V_2O_5–UO_3,[152] Bi_2O_3–V_2O_5–TiO_2,[143] and Bi_2O_3–V_2O_5–ZnO,[142] for example.

3.10 Bi_2O_3–MO (M = Ca, Sr, Ba, and Pb)

Figure 23 shows the typical Bi_2O_3–CaO phase equilibrium diagram.[153,154] It can be seen that the domain of the α-fcc solid solution does not extend below 680°C, while the γ-bcc solid solution is not stable below 800°C. Only the β-rhombohedral solid solution is stable over a wide range of temperature. Similar phases are observed in the SrO-doped and BaO-doped systems with a number of minor differences.[1,38,155] The γ-phase in the SrO doped system is tetragonal, with the Bi and Sr ions ordered on different sites of the tetragonal space group I4/m. The appearance of the β-phase in all three systems has allowed for a number of papers to have been published on the 3 dopants.

Boivin and Thomas[153] showed that the unit cell parameters (in Å) of $Bi_{1-x}M_xO_{1.5\text{-}x/2}$ are as shown in Table 10.

The authors also showed that the layers of cations are stacked along the c-axis with the following sequence; –Bi–Bi–(M, Bi)–Bi–Bi–(M, Bi)–. Two kinds of oxide ions were detected inside the blocks consisting of a mixed layer surrounded by two Bi layers. The conduction properties were ascribed to the migration of the remaining anions in the space between two successive Bi layers. The authors also produced conductivity curves for Ca and Ba-doped systems, and showed that the Ca had the superior oxygen ion conductivity (approximately 1 S cm^{-1} at T > 1000 K). Boivin and Thomas,[156] using XRD on single crystals of $Bi_{1-x}M_xO_{1.5-x/2}$ (M = Ca, Ba, Sr), suggested the existence of conduction planes, and the preservation of the cation network. Conflant *et al.*[154] delineated the Bi_2O_3–CaO system in terms of 4 incongruently melting compounds ($Bi_{14}Ca_5O_{26}$, Bi_2CaO_4, $Bi_{10}Ca_7O_{22}$ and $Bi_6Ca_7O_{16}$), and the four solid solutions described above (fcc, bcc and two rhombohedral (β_1 and β_2)).

Conflant *et al.*[154] described how the β_1 to β_2 transition (observed in the phase equilibrium diagrams for CaO, SrO and BaO doped Bi_2O_3) does not alter the cationic stacking. The early work of Takahashi *et al.*[38,53] suggested that $Bi_{1-x}M_xO_{1.5-x/2}$ (M = Ba, Sr, and Ca) is a good anionic conductor; the results have been described in an earlier section.

Suzuki *et al.*[158] investigated the system $(BaO)_x(Bi_2O_3)_{1-x}$ with Ag or Pt paste electrodes. The authors observed that the electrode conductance varied with oxygen partial pressure $PO_2 \propto PO_2^{0.362}$ at 450°C in the PO_2 region of 1–10^{-5} atm, for the Ag paste electrode.

Sillen and Aurivillius[159] showed that the system Bi_2O_3–SrO had a wide range of solid solutions; the solid solution was ascribed a rhombohedral lattice structure, later confirmed to be correct by a number of other authors as described above.

Figure 24 shows a typical conductivity plot of $Bi_{1-x}M_xO_{1.5\text{-}x/2}$ (M = Ba, Sr, and Ca). At lower temperatures, the conductivity of $Bi_{1-x}Ca_xO_{1.5-x/2}$ was found to be less than that of $Bi_{1-x}M_xO_{1.5-x/2}$. This was explained by Takahashi *et al.*[38] to be due to the cation size effect; the radius of Ca^{2+} is smaller than Sr^{2+}. A common feature of these systems, is the abrupt jump in conductivity at approximately 600°C. This was attributed to the β_1 to β_2 transition within the rhombohedral phase. BaO was observed as having the lowest transition temperature, and one of the highest ionic conductivities of the Bi_2O_3-based systems; 8.8×10^{-1} S cm^{-1} at 600°C for 16 mol% BaO doped Bi_2O_3.[160]

In this section of MO doped Bi_2O_3, special mention should be made to the PbO-doped Bi_2O_3 systems as a lot of work has recently been undertaken

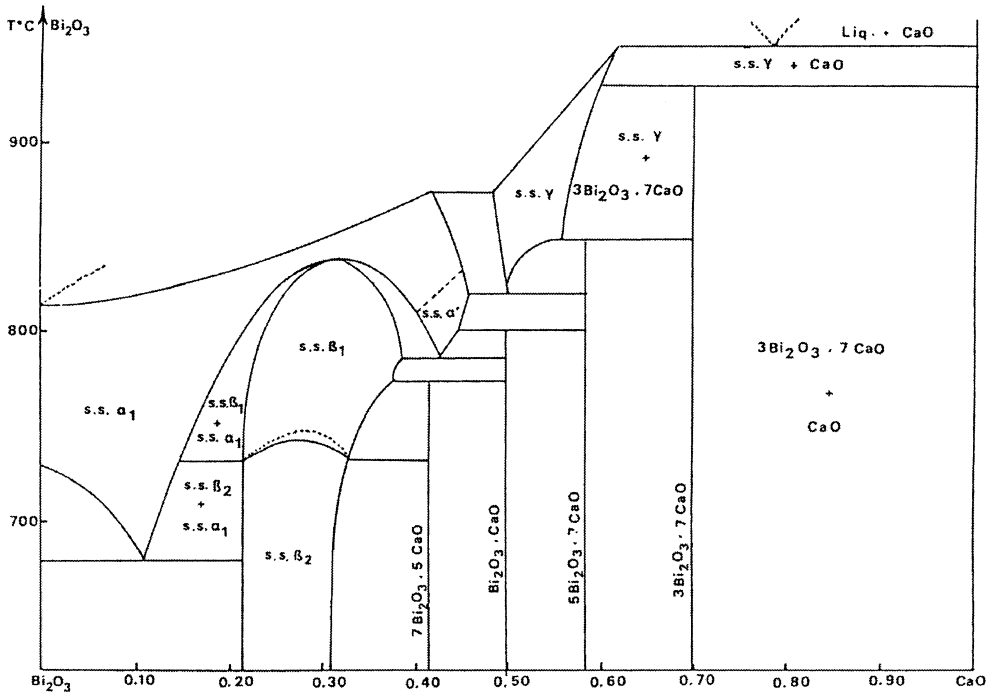

Fig. 23. Sub-solidus phase diagram of the system Bi_2O_3–CaO (Ref. 153).

Table 10. Unit cell parameters (in Å) for $Bi_{1-x}M_xO_{1.5-x/2}$ where M = Ca, Sr and Ba

	M = Ca	*M = Sr*	*M = Ba*
x	0·13	0·235	0·156
a	3·950	3·971	4·006
c	27·87	28·42	28·58

on this material. Early work carried out by Levin and Roth[1] suggested that a bcc structure could be stabilised at low PbO dopant concentrations, while Sillen and Aurivillius[159] showed the presence of a tetragonal phase, with a very broad homogeneity area, ranging from about 29 to about 53% Pb (as a percentage of Pb in the total number of metal ions). The original Bi_2O_3–PbO phase equilibrium diagrams,[161–164] reported, used powder X-ray diffraction analysis on bulk materials. The results were, in part, misleading and it was not clear whether the data was obtained from quenching the sample or from equilibrium cooling. The latest work was performed by Sammes *et al.*,[165] and the phase equilibrium diagram is shown in Fig. 25. Sammes *et al.*[165] used powder X-ray diffraction, Raman spectroscopy and infrared spectroscopy to analyse the bulk samples after having been quenched from a range of temperatures. All the phase equilibrium diagrams showed the following features. Above approximately 590°C (although this depends upon the PbO concentration) a bcc phase (β) is present, and is stable over a wide range of homogeneity (approximately 30–70 mol%). The high temperature bcc form cannot be quenched in and transforms, on cooling, into either a tetragonal β_2-phase (at dopant concentrations greater than 50 mol%) or a monoclinic β_1-phase. At 55·55 mol% PbO, tetragonal-β_2, (lattice parameters of $a = 4{\cdot}041(1)$ Å, and $c = 5{\cdot}023(1)$ Å) were found to be stable between room temperature and 450°C. Between 450 and 590°C, the β_2-phase starts to decompose into the definite compound β-$Bi_8Pb_5O_{17}$ with the bcc structure, via a mixed phase. Honnart *et al.*[166] also showed that the ionic conductivity of $Bi_8Pb_5O_{17}$ was in excess of 1 S cm^{-1} at temperatures greater than 590°C, after the provisional work of Boivin,[167] and Demonchy *et al.*,[168] who showed that the high temperature bcc phase was a good ionic conductor. Sammes *et al.*[169] investigated the ionic conductivity of $(Bi_{1-x}Sb_x)_8Pb_5O_{17}$ ($x = 0$–0.2). With increase in x, the temperature at which the β_2-phase decomposed into the mixed phase was reduced, but an increase in the temperature of the β-phase formation resulted. The ionic conductivity data, as a function of temperature, is shown in Fig. 26. The authors also noted that the ionic conductivity of the β-phase altered when Sb_2O_3 was changed for the oxides of Tm, Gd, or Dy, although not a large effect, the conductivity increased in the order Dy > Gd > Tm > Sb in the system examined, at a level of 10 mol% dopant. The effect of Sb_2O_3 on the mechanical properties has been examined, and has been shown to greatly increase both the modulus of rupture and the fracture toughness of the material;[170]

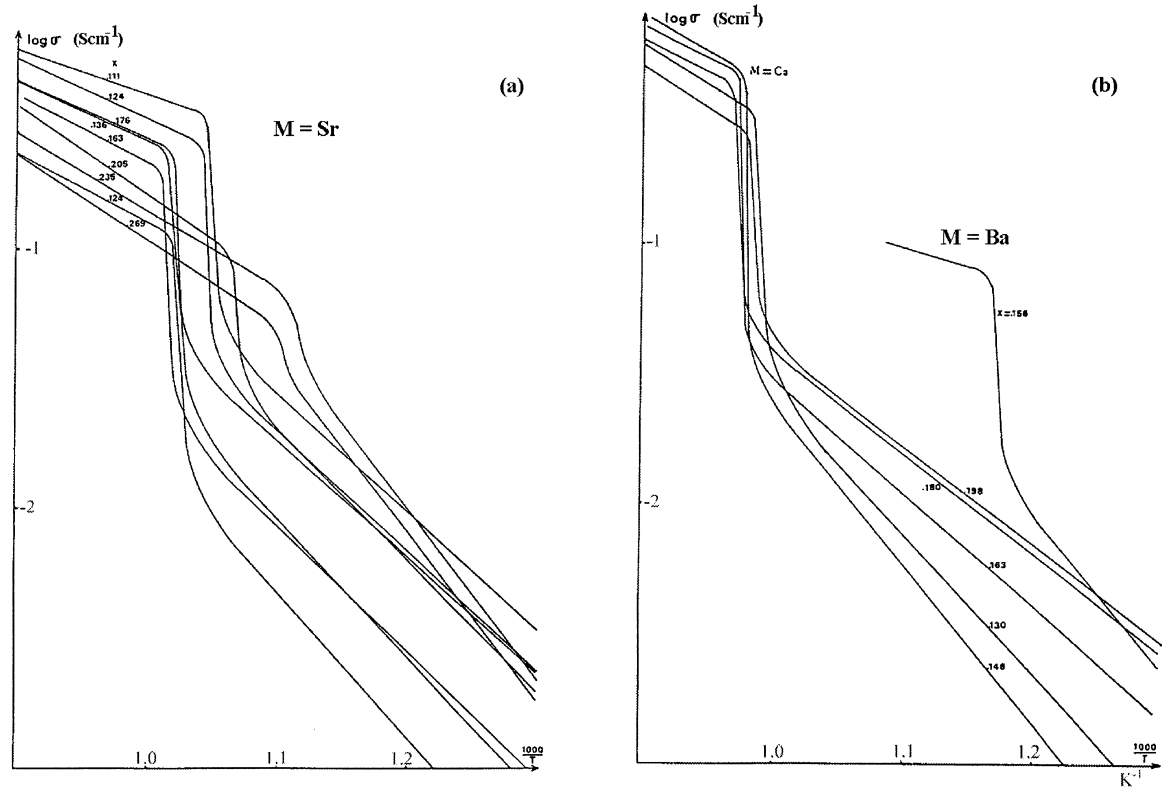

Fig. 24. Conductivity of $Bi_{1-x}M_xO_{1\cdot5-x/2}$ (a) (M = Sr) rhombohedral solid solutions; (b) (M = Ba, Ca) rhombohedral solid solutions (Ref. 153).

this is quite an important issue as the mechanical integrity of $Bi_8Pb_5O_{17}$ was shown to be very poor.

As has been stated above, the highly conductive β-phase is not stable below approximately 590°C, and cannot be quenched in. The phase transition from the β-phase to the β_2-phase, on cooling $Bi_8Pb_5O_{17}$ to room temperature, is via a series of intermediates which have been labelled ϕ by Fee *et al.*[171] the authors also found, that ϕ could be stabilised to room temperature. When $Bi_8Pb_5O_{17}$ was heated to below 470°C, or heated above 590°C, and cooled to room temperature, the tetragonal β_2-phase was formed. However, when the material was re-heated to intermediate temperatures, and cooled to room temperature, the intermediate ϕ-phase was observed. The authors suggested that the thermal expansion of ϕ matches that of stainless steel and MgO, and could, therefore, be used in the fabrication of thin supported membranes. Raman spectra also confirmed these findings.[172]

Sammes *et al.*[173] showed the effect of oxygen partial pressure on the conductivity of $(Bi_{1-x}Sb_x)_8Pb_5O_{17}$. They described how the oxygen ion domain (the partial pressure of oxygen at which the electronic and ionic conductivities are equal) increased from approximately 10^{-11} atms of oxygen at $x=0$, to 10^{-13} atms of oxygen, at $x=0\cdot1$. At $x>0\cdot1$, the ionic domain was found to drop off again. Sammes *et al.*[174] observed two room temperature phases in $Bi_8Pb_5O_{17}$, rather than just one. They noticed that as well as β_2, a second phase, $Bi_{1\cdot23}Pb_{0\cdot77}O_{2\cdot62}$ (labelled β_3) was always present; in fact the authors showed that a third phase, $Bi_6Pb_2O_{11}$ could also be produced when ethanol was used as a milling medium. For the system $(Bi_{1-x}Sb_x)_8Pb_5O_{17}$, the phase Bi_3SbO_7 was present at Sb_2O_3 concentrations greater than 2·5 mol%. The phase equilibrium for this system was later investigated by Sammes and Du.[175] Dumelie *et al.*[176] discussed the suitability of $Bi_{0\cdot571}Pb_{0\cdot428}O_{1\cdot285}$ as an oxygen separation membrane, due to its high conductivity at low temperature. The authors observed that the material was quite weak, and that the mechanical properties could be enhanced by making a composite with zirconia. The optimised membrane was capable of operating continuously up to 300 mA cm^{-2} at 600°C. Fee and Long[177] described how $Bi_8Pb_5O_{17}$ could be doped with a metallic element such as Ni or Cu, and produce a single phase mixed ionic/electronic electrolyte with an ionic conductivity close to that of the original material. The ionic transference number (t_i) was observed to be between 0·5 and 0·9, dependant upon the dopant concentration. The authors considered that the material could be used as an oxygen separation membrane, without the requirement for electrodes. This was a very useful feature because, as discussed by Bettahar *et al.*,[178] platinum metal reacts with $Bi_8Pb_5O_{17}$ to form a ternary BiPbPt oxide.

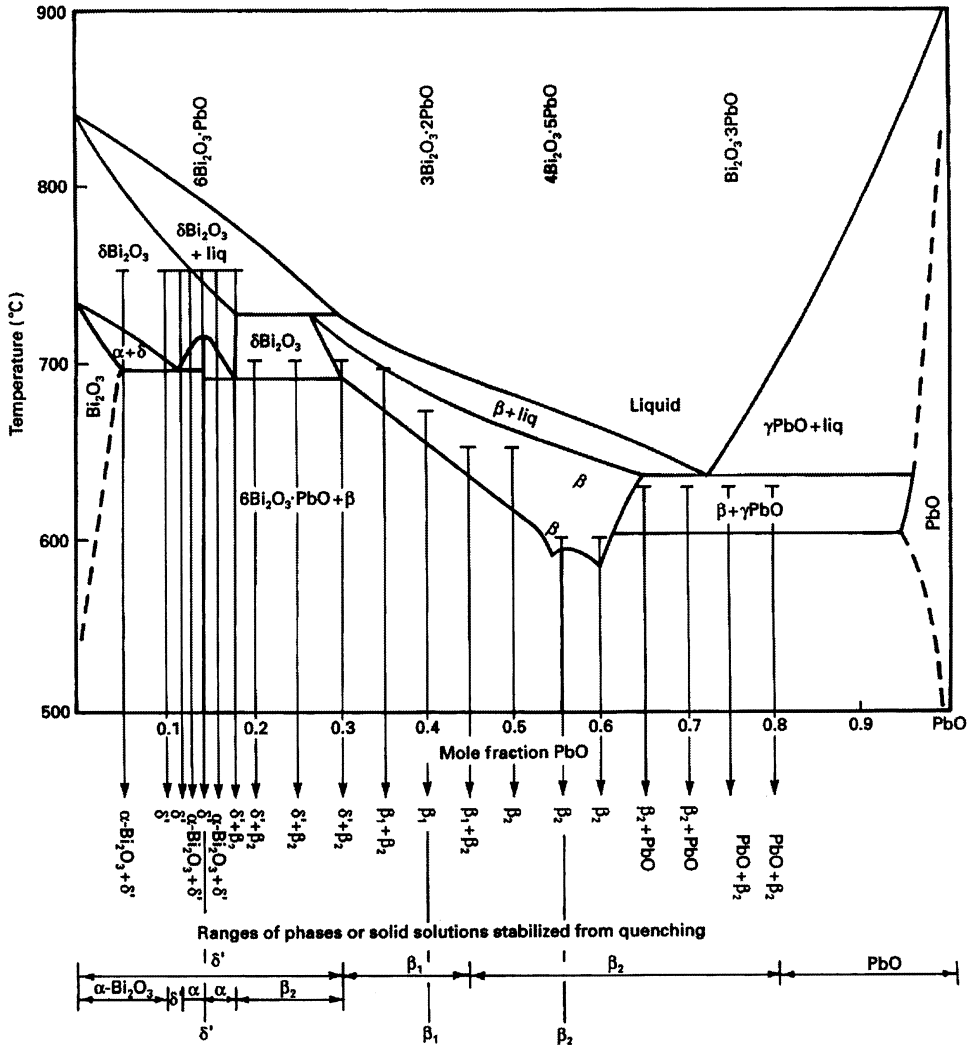

Fig. 25. Temperature/composition phase diagram of the system $(Bi_2O_3)_{1-x}(PbO)_x$, with specific quench lines and stabilised room-temperature phase ranges (Ref. 165).

Other ternary systems have been examined including Bi_2O_3–Y_2O_3–PbO[179] and Bi_2O_3–CaO–PbO, which are also mixed oxides.[180] Omari and co-workers[180,181] observed that the Pb^+ ion could be used as a very good stabiliser for the high temperature modification, δ-Bi_2O_3.

3.11 Other doped Bi_2O_3 systems

Bi_2O_3–MoO_3 has been studied, and has been found to have relatively high oxygen ion conductivity.[181,182] Takahashi *et al.*[181] found the Bi_2O_3–MoO_3 system to be stable as a tetragonal phase between 22 and 28 mol% MoO_3. The authors showed that the tetragonal phase was the conducting phase. Above approximately 30 mol% MoO_3, the system was found to be predominantly monoclinic, with poor ionic conductivity. The compound $Bi_6Mo_2O_{15}$ has been studied in great detail by Boon and Metselaar,[183] who showed that there are two modifications of the compound, a high temperature and a low temperature form. However, the authors found that the material was not stable over a long period of time, and thus they

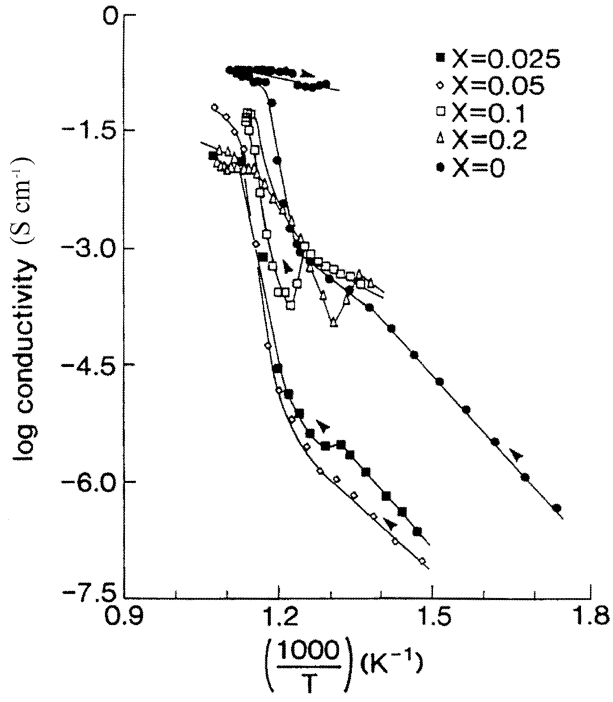

Fig. 26. Oxygen ionic conductivity, as a function of temperature, for the $(Bi_{1-x}Sb_x)_8Pb_5O_{17}$ sample (Ref. 169).

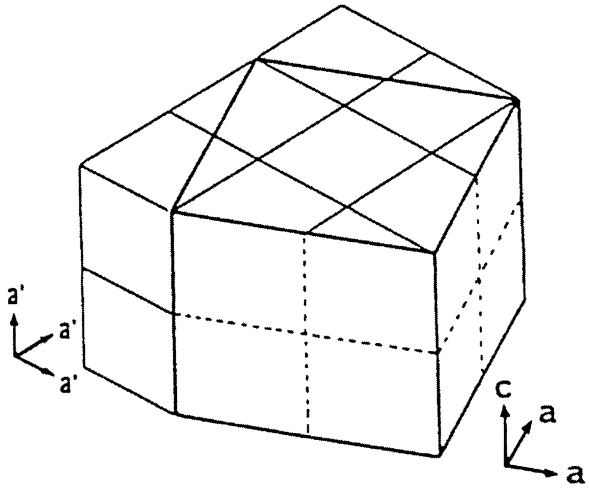

Fig. 27. Schematic representation of the relations of the unit cell axes of solid solution having the $7Bi_2O_3{\cdot}2WO_3$ structure. Heavy solid lines indicate the tetragonal cell (a,c) and weak solid lines outline the pseudo-fcc subcells (a′), where a′∼5·6 Å, a∼$\sqrt{}$5a′, and c∼2a′ (Ref. 187).

Table 11. Crystal structure and the conductivity at 600°C, for the samples of doped bismuth oxides examined by Esaka *et al.*[186]

M *in* $(Bi_2O_3)_{1-x}(MO_2)_x$	x *in* $(Bi_2O_3)_{1-x}(MO_2)_x$	*Crystal form*	*Conductivity at 600°C (S cm^{-1})*
Te	0·33	Rhomb + Mon	2×10^{-4}
Te	0·46	Rhomb + Mon	$1{\cdot}7\times10^{-4}$
Te	0·57	Rhomb	$1{\cdot}1\times10^{-3}$
Te	0·67	Tetrahedral	$2{\cdot}7\times10^{-3}$
Ti	0·57	Orthorhombic + x	$5{\cdot}1\times10^{-5}$
Ti	0·67	Orthorhombic + x	4×10^{-5}
Sn	0·57	Cubic + x	$7{\cdot}3\times10^{-4}$
Sn	0·67	Cubic + x	$1{\cdot}7\times10^{-4}$
Zr	0·57	Tetrahedral + x	$5{\cdot}6\times10^{-4}$
Zr	0·67	Tetrahedral + x	3×10^{-4}
Zr	0·75	Tetrahedral + x	3×10^{-4}

Rhom = Rhombohedral, Mon = Monoclinic, and x = Unknown.

suggested that it was not an appropriate material for use in an electrochemical device.

Hoda and Chang[184] have published the latest phase equilibrium data for Bi_2O_3–WO_3, and have shown that there are 4 intermediate phases present: $(Bi_2O_3)_7(WO_3)$, $(Bi_2O_3)_7(WO_3)_2$, $(Bi_2O_3)(WO_3)$, and $(Bi_2O_3)(WO_3)_2$. $(Bi_2O_3)_7(WO_3)$ is tetragonal at room temperature, and transforms to the fcc structure at 784°C, while $(Bi_2O_3)_7(WO_3)_2$ (22·22 mol% WO_3) was shown to exist in the fcc δ-form (with an extensive solid solution range) at room temperature. However, Watanabe[60] suggested that the tetragonal unit cell consists of pseudo-fcc subcells, as shown in Fig. 27 then the phase was erroneously identified as the stabilised δ-phase; thus, the author suggests, δ-Bi_2O_3 cannot be stabilised in this system. Watanabe *et al.*[185] also revealed that the phase $(Bi_2O_3)_7(WO_3)_2$ crystallises in the tetragonal symmetry with the space group $I4_1/a$.

Takahashi and Iwahara[63] investigated the ionic properties of $(Bi_2O_3)_{1-x}(WO_3)_x$ ($x = 0{\cdot}05$–$0{\cdot}5$), and found very high oxygen ion conduction in the fcc structure. $(Bi_2O_3)_{0{\cdot}78}(WO_3)_{0{\cdot}22}$, for example, was shown to have an ionic conductivity of $1{\cdot}5\times10^{-1}$ S cm^{-1} at 880°C, with an oxygen transport number close to unity (down to at least 10^{-15} atm oxygen partial pressure).

Bi_2O_3–Pr_6O_{11} has also been studied in detail by Esaka *et al.*[186] and Sammes and Gainsford.[187] The material was found to have oxide ion conductivity in the rhombohedral β-phase, present at compositions less than 35 mol% $Pr_2O_{11/3}$. *P*-type conductivity was observed in compositions containing more than 40 mol% $Pr_2O_{11/3}$, (where the rhombohedral phase was of the type LaOF) and was thought to be due to a change in the oxidation state of the Pr ion. The mixed conductivity was also observed by Shuk *et al.*,[188] at concentrations greater than 50 mol% $Pr_2O_{11/3}$.

Other systems that that are worth mentioning include: Bi_2O_3–TiO_2, Bi_2O_3–SnO_2, Bi_2O_3–ZrO_2, Bi_2O_3–TeO_2, and Bi_2O_3–Re_2O_7. Esaka *et al.*[189] examined the oxide ion conductivity in Bi_2O_3–MO_2 (M = Ti, Sn, Zr, and Te), and observed that at all the compositions employed, the δ-phase could not be stabilised. Table 11 summarises the crystal form and the conductivity at 600°C, for the samples examined by Esaka *et al.*[186]

Thus, all the samples showed low conductivity, in fact this was observed at all temperatures below 700°C.

Recently, Bi_2O_3–Re_2O_7 was studied[190] as a possible electrolyte material, and the system $Bi_{2x}Re_xO_{3+2x}$ was observed as having a defect-fluorite structure, however the conductivity was not examined in this work.

4 Conclusions

This paper has summarised the literature on the conductivity, structure and properties of the doped-Bi_2O_3 system. Doped-Bi_2O_3 is a very interesting material, and forms a vast array of solid solutions, having very high oxygen ion conductivity's, with many other metal oxides (MO, M_2O_3, M_2O_5, for example), although the system studied in most detail is that of Bi_2O_3–M_2O_3 (M = Y or a rare earth oxide). Most of the Bi_2O_3–M_2O_3 solid solutions are either fcc δ-Bi_2O_3, or rhombohedral, depending upon the dopant type. However, as has been shown, it is quite apparent

that there is some controversy over the stability of δ-Bi_2O_3, and a lot of the provisional work showing that the system could be stabilised to room temperature has been disputed in later work. Whether δ-Bi_2O_3 can be stabilised to room temperature or not, does not alter the fact that Bi_2O_3–Er_2O_3, for example, has been shown to have one of the highest oxygen ion conductivities of the doped-Bi_2O_3 systems in air; approximately $0{\cdot}4\,S\,cm^{-1}$ could be realised at 973 K for $(Bi_2O_3)_{0{\cdot}8}(M_2O_3)_{0{\cdot}2}$, postulated as being due to the low value of dopant necessary for stabilising the fcc δ-Bi_2O_3 (although this latter statement is still under scrutiny).

A number of other doped-Bi_2O_3 were examined in this paper, however, a new family known as BIMEVOX and Aurivillius phases are worth mentioning. These are based on $Bi_4V_2O_{11}$, with a metal ion (Cu or Ni, for example) replacing some of the V in solid solution. $Bi_2V_{0{\cdot}9}Cu_{0{\cdot}1}O_{5{\cdot}35}$, for example, was found to have an oxygen ion conductivity of $3\times10^{-3}\,S\,cm^{-1}$ at 510 K.

Finally, the paper examines some of the newer systems, and shows that the structures are very complex, although a lot of exciting work is still being undertaken to try and realise a stable high oxygen ion conductor.

References

1. Levin, E. M. and Roth, R. S., Polymorphism of bismuth sesquixide. II. Effect of oxide additions on the polymorphism of Bi_2O_3. *Journal of Research of the National Bureau of Standards-A*, 1964, **68A**, 189–206.
2. Guertler, W., Über Wismutoxyd. *Zeitschrift fur Anorganische Chemie*, 1903, **37**, 222–224.
3. Belladen, L., Il sistema Bi_2O_3–PbO. *Gazzetta Chimica Italiana*, 1922, **52**, 160–164.
4. Sillen, L. G., X-ray studies of bismuth trioxide. *Arkiv för Kemi, Mineralogi och Geologi*, 1937, **12A**, 1–15.
5. Schumb, W. C. and Rittner, E. S., *Journal of the American Chemical Society*, 1943, **65**, 1055–1060.
6. Gattow, G. and Schroder, H., Die Kristallsttruker der hochtemperaturemodifikation von Wismut (III)-oxid (δ-Bi_2O_3). *Zeitschrift für Anorganishe und Allgemeine Chemie*, 1962, **318**, 176–189.
7. Aurivillius, B. and Sillen, L. G., Polymorphy of bismuth trioxide. *Nature (London)*, 1945, **155**, 305–306.
8. Gattow, G. and Schutze, D., Über ein Wismut(III)-oxid mit höherm sauerstoffgehalt (β-modifikation). *Zeitschrift für Anorganishe und Allgemeine Chemie*, 1964, **328**, 44–68.
9. Rao, C. N. R., Subba Rao, G. V. and Ramdas, S., Phase transformations and electrical properties of bismuth sesquioxide. *Journal of Physical Chemistry*, 1969, **73**, 672–675.
10. Matsuzaki, R., Masumizu, H. and Saeki, Y., Phase transition of bismuth (III) oxide on cooling. *Denki Kagaku Oyobi Kogyo Butsuri*, 1974, **42**(11), 578–581.
11. Matsuzaki, R., Masumizu, H. and Saeki, Y., Phase transition of bismuth (III) oxide prepared by the thermal decomposition of bismuth sulfate. *Bulletin of the Chemical Society of Japan*, 1975, **48**(11), 3397–3384.
12. Levin, E. M. and McDaniel, C. L., Heat of transformation in Bi oxide determined by differential thermal analysis (DTA). *Journal of Research National Bureau of Standards Section A*, 1965, **69**(3), 237–243.
13. Levin, E. M. and McDaniel, C. L., The system Bi_2O_3–B_2O_3. *Journal of the American Ceramic Society*, 1962, **45**, 355–360.
14. Kelley, K. K., Contributions to the data on theoretical metullurgy. V. Heats of fusion of inorganic substances. *United States Department of the Interior, Bureau of Mines, Bulletin*, 1936, **393**, 1–66.
15. Harwig, H. A. and Gerards, A. G., The polymorphism of bismuth sesquioxide. *Thermochimica Acta*, 1979, **28**, 121–131.
16. Sillen, L. G., The crystal structure of monoclinic α-Bi_2O_3. *Naturwissenschaften*, 1940, **28**, 206–207.
17. Sillen, L. G., Crystal structure of monoclinic α-Bi_2O_3. *Zeitschrift Kristallographie*, 1941, **A103**, 274–290.
18. Malmos, G., Crystal structure of α-bismuth trioxide. *Acta Chemica Scandinavia*, 1970, **24**, 384–396.
19. Harwig, H. A., On structure of bismuth sesquioxide: the α, β, γ, and δ-phase. *Zeitschrift für Anorganishe und Allgemeine Chemie*, 1978, **444**, 151–166.
20. Malmos, G. and Thomas, J. O., Least squares refinement based on profile analysis of powder film intensity data measured on an automatic microdensitomer. *Journal of Applied Crystallography*, 1977, **10**, 7–11.
21. Cheetham, A. K. and Taylor, J. C., Profile analysis of powder neutron diffraction data: its scope, limitations, and applications in solid state chemistry. *Journal of Solid State Chemistry*, 1977, **21**, 253–275.
22. Harwig, H. A. and Weenk, J. W., Phase relations in bismuth sesquioxide. *Zeitschrift für Anorganishe und Allgemeine Chemie*, 1978, **444**, 167–177.
23. Willis, B. T. M., The anomalous behavior of the neutron reflections of fluorite. *Acta Crystallographica*, 1965, **18**, 75–76.
24. Willis, B. T. M., Neutron diffraction studies of the actinide oxides II: thermal motions of the atoms in uranium dioxide and thorium dioxide between room temperature and 1100°C. *Proceedings of the Royal Society*, 1963, **A274**, 134–144.
25. Verkerk, M. J. and Burggraaf, A. J., High oxygen ion conduction in sintered oxides of Bi_2O_3-Ln_2O_3 system. *Solid State Ionics*, 1981, **3/4**, 463–467.
26. Zav'yalova, A. A. and Imamov, R. M., Cubic structure of δ-bismuth sesquioxide. *Kristallografiya*, 1969, **14**, 331–333.
27. Medernach, J. W. and Snyder, R. L., Powder diffraction patterns and structure of the bismuth oxides. *Journal of the American Ceramic Society*, 1978, **61**, 494–497.
28. Kilner, J. A. and Faktor, J. D. In *Progress in Solid Electrolytes*, eds T. A. Wheat, A. Ahmad and A. K. Kuriakose. Canada Centre for mineral and Energy Technology, Ottawa, 1983, p. 347.
29. Jacobs, P. W. M. and Mac Donaill, D. A., Computer simulation of δ-bismuth oxide. *Solid State Ionics*, 1986, **18&19**, 209–213.
30. Jacobs, P. W. M. and Mac Donaill, D. A., Computational simulation of δ-Bi_2O_3. I. Disorder. *Solid State Inonics*, 1987, **23**, 279–293.
31. Jacobs, P. W. M. and Mac Donaill, D. A., Computational simulation of δ-Bi_2O_3. II. Charge migration. *Solid State Ionics*, 1987, **23**, 295–305.
32. Jacobs, P. W. M. and Mac Donaill, D. A., Computational saimulation of δ-Bi_2O_3. III. A comparative study of static lattice models. *Solid State Ionics*, 1987, **23**, 307–318.
33. Shuk, P., Wiemhofer, H.-D., Guth, U., Gopel, W. and Greenblatt, M., Oxide ion conducting electrolytes based on Bi_2O_3. *Solid State Ionics*, 1996, **89**, 179–196.
34. Mac Donaill, D. A. and Jacobs, P. W. M., On the lattice-parameter of some sesquioxides with the fluorite structure. *Journal of Solid State Chemistry*, 1990, **84**, 183–193.
35. Koto, K., Suda, K., Ishizawa, N. and Maeda, H., Oxide ion motion in bismuth sesquioxide (δ-Bi_2O_3). *Solid State Ionics*, 1994, **72**, 79–85.

36. Mansfield, R., The electrical properties of bismuth oxide. *Proceedings of the Physical Society, London*, 1949, **62B**, 478–483.
37. Hauffe, K. and Peters, H., Conductivity measurements in the system bismuth (III) oxide. *Zeitschrift fuer Physikalische Chemie*, 1952, **201**, 121–209.
38. Takahashi, T., Iwahara, H. and Nagai, Y., High oxide ion conduction in sintered bismuth oxide containing strontium oxide, calcium oxide, or lanthanum oxide. *Journal of Applied Electrochemistry*, 1972, **2**, 97–104.
39. Harwig, H. A. and Gerards, A. G., Electrical properties of the α, β, γ, and δ phases of bismuth sesquioxide. *Journal of Solid State Chemistry*, 1978, **26**, 265–274.
40. Shuk, P. and Mobius, H.-H., Oxide-ion conducting electrolytes. 40. Transport numbers and electrical conductivity of modifications of bismuth (III) oxide. *Zeitschift fuer Physikalische Chemie*, 1985, **266**, 9–16.
41. Mairesse, G., In *Fast Ion Transport in Solids*, ed. B. Scrosati, Kluver, Amsterdam, 1993, p. 271.
42. Laarif, A. and Theobald, F., The lone pair concept and the conductivity of bismuth oxides Bi_2O_3. *Solid State Ionics*, 1986, **21**, 183–193.
43. Kamijo, N., Kageyama, H., Koto, K., Maeda, H., Hida, M., Ishida, T. and Terauchi, H., Edge and EXAFS studies of bismuth oxide-yttrium oxide (Bi_2O_3–Y_2O_3) oxygen conductor. *Journal of the Physical Society of Japan*, 1986, **55**, 2217–2231.
44. Battle, P. D., Catlow, C. R. A., Chadwick, A. V., Cox, P., Greaves, G.N. and Moroney, L. M., Structural and dynamical studies of δ-Bi_2O_3 oxide ion conductors. *Journal of solid State Chemistry*, 1987, **69**, 230–239.
45. Koto, K., Ito, H., Kanamaru, F., Emura, S. and Yoshiasa, A., EXAFS study of the fluorite-type compounds in the system Bi_2O_3–Gd_2O_3. *Solid State Ionics*, 1990, **40/41**, 288–292.
46. Iwahara, H., Esaka, T., Sato, T. and Takahashi, T., Formation of high oxide ion conductive phases in the sintered oxides of the system Bi_2O_3–Ln_2O_3 (Ln = La–Yd). *Journal of Solid State Chemistry*, 1981, **39**, 173–180.
47. Shannon, R. D. and Prewitt, C. T., Effective ionic radii in oxides and fluorides. *Acta Crystallographica*, 1969, **B25**, 925–946.
48. Datta, R. K. and Meehan, J. P., The system Bi_2O_3–R_2O_3 (R = Y, Gd). *Zeitschrift für Anorganishe und Allgemeine Chemie*, 1971, **383**, 328–337.
49. Gattow, G. and Schroder, H., Bismuth oxide. III. The crystal structure of the high temperature modification of bismuth (III) oxide (δ-Bi_2O_3). *Zeitschrift für Anorganishe und Allgemeine Chemie*, 1962, **318**, 176–189.
50. Takahashi, T., Iwahara, H. and Arao, T., High oxide ion conducting in sintered oxides of the system bismuth (III) oxide-yttrium oxide. *Journal of Applied Electrochemistry*, 1975, **5**, 187–195.
51. Takahashi, T. and Iwahara, H., Oxide ion conductors based on bismuth sesquioxide. *Materials Research Bulletin*, 1978, **13**, 1447–1453.
52. Verkerk, M. J. and Burggraaf, A. J., Free energy of formation of stabilized Bi_2O_3 (fcc) from e.m.f measurements. *Journal of Applied Electrochemistry*, 1980, **10**, 677–681.
53. Takahashi, T., Esaka, T. and Iwahara, H., Conduction in bismuth (III) oxide-based oxide ion conductors under low oxygen pressure. I. Current blackening of the bismuth (III) oxide-yttrium oxide electrolyte. *Journal of Applied Electrochemistry*, 1977, **7**, 299–302.
54. Lawless, W. N. and Swartz, S. L., Thermal properties of a bismuth oxide (Bi_2O_3)–yttrium oxide (Y_2O_3) oxygen conductor at low temperatures. *Physical Review*, 1983, **B28**, 2125–2129.
55. Wang, C., Xu, X. and Li, B., Ionic and electronic conduction of oxygen ion conductors in the Bi_2O_3–Y_2O_3 system. *Solid State Ionics*, 1984, **13**, 135–140.
56. Joshi, A. V., Kulkarni, S., Nachlas, J., Diamond, J. and Weber, N., Phase-stability and oxygen transport characteristics of yttria-stabilized and niobia-stabilized bismuth oxide. *Journal of Materials Science*, 1990, **25**, 1237–1245.
57. Watanabe, A. and Kikuchi, T., Cubic-hexagonal transformation of yttia–stabilized δ-bismuth sesquioxide, $Bi_{2-2x}Y_{2x}O_3$ ($x = 0{\cdot}215$–$0{\cdot}235$. *Solid State Ionics*, 1986, **21**, 287–291.
58. Kruidhof, K., DeVries, K. J. and Burggraaf, A. J., Thermochemical stability and non-stoichiometry of yttria-stabilized bismuth oxide solid-solutions. *Solid State Ionics*, 1990, **37**, 213–215.
59. Dodor, P. J., Tanaka, J. and Watanabe, A., Electrical characterization of phase transition in yttrium doped bismuth oxide, $Bi_{1{\cdot}55}Y_{0{\cdot}45}O_3$. *Solid State Ionics*, 1987, **25**, 177–181.
60. Watanabe, A., Is it possible to stabilize δ-Bi_2O_3 by an oxide additive? *Solid State Ionics*, 1990, **40/41**, 889–892.
61. Dordor, P. J., Tanaka, J. and Watanabe, A., Electrical characterization of phase transition in yttrium doped bismuth oxide, $Bi_{1{\cdot}55}Y_{0{\cdot}45}O_3$. *Solid State Ionics*, 1987, **25**, 177–181.
62. Watanabe, A., Phase equilibria in the system Bi_2O_3–Y_2O_3: no possibility of δ-Bi_2O_3 stabilization. *Solid State Ionics*, 1996, **86–88**, 1427–1430.
63. Takahashi, T. and Iwahara, H., High oxide ion conduction in sintered oxides of the system bismuth oxide–tungsten oxide. *Journal of Applied Electrochemistry*, 1973, **3**, 65–72.
64. Takahashi, T., Esaka, T. and Iwahara, H., High oxide ion conduction in the sintered oxides of the system bismuth (III) oxide–gadolinium (III) oxide. *Journal of Applied Electrochemistry*, 1975, **5**, 197–202.
65. Takahashi, T., Esaka, T. and Iwahara, H., Electrical conduction in the sintered oxides of the bismuth oxide–barium oxide systems. *Journal of Solid State Chemistry*, 1976, **16**, 317–323.
66. Battle, P. D., Catlow, C. R. A., Heap, J. W. and Moroney, L. M., Structural and dynamical studies of δ-Bi_2O_3 oxide ion conductors I. The structure of $(Bi_2O_3)_{1-x}(Y_2O_3)_x$ as a function of x and temperature. *Journal of Solid State Chemistry*, 1986, **63**, 8–15.
67. Battle, P. D., Catlow, C. R. A., Drennan, J. and Murray, A. D., The structural properties of the oxygen conducting δ phase of Bi_2O_3. *Journal of Physics*, 1983, **C16**, L561–566.
68. Infante, C. E., Gronemeyer, C. and Li, F., Neutron diffraction study of the oxide conducting δ^*-phase of $(Bi_2O_3)_{1-x}(Y_2O_3)_x$ ($x = 0{\cdot}25$). *Solid State Ionics*, 1987, **25**, 63–70.
69. Jurado, J. R., Moure, C., Duran, P. and Valverde, N., Preparation and electrical properties of oxygen ion conductors in the Bi_2O_3–Y_2O_3(Er_2O_3). *Solid State Ionics*, 1988, **28–30**, 518–523.
70. Duran, P., Jurado, J. R., Moure, C., Valverde, N. and Steele, B. C. H., High oxygen ion conduction in some bismuth sesquioxide-yttrium sesquioxide (erbium sesquioxide) solid solutions. *Materials Chemistry and Physics*, 1987, **18**, 287–294.
71. Wachsman, E. D., Jiang, N., Mason, D. M. and Stevenson, D. A., In *SOFC* I, ed. S. C. Singhal, Electrochem. Soc. Proc. Vol. 89–11, 1989, 15.
72. Waschsman, E. D., Ball, G. R., Jiang, N. and Stevenson, D. A., Structural and defect studies in solid oxide electrolytes. *Solid State Ionics*, 1992, **52**, 213–218.
73. Fung, K. Z., Beak, H. D. and Virkar, A. V., Thermodynamic and kinetic considerations for Bi_2O_3-based electrolytes. *Solid State Ionics*, 1992, **52**, 199–211.
74. Meng, G., Chen, C., Han, X., Yang, P. and Peng, D., Conductivity of Bi_2O_3-based oxide ion conductors with double stabilizers. *Solid State Ionics*, 1988, **28–30**, 533–538.
75. Berezovsky, J., Liu, H. K. and Dou, S. X., Conductivity and microstructure of bismuth oxide-based electrolytes

with enhanced stability. *Solid State Ionics*, 1993, **66**, 201–206.
76. Huang, K., Feng, M. and Goodenough, J. B., Bi_2O_3-Y_2O_3-CeO_2 solid solution oxide-ion electrolyte. *Solid State Ionics*, 1996, **89**, 17–24.
77. Fung, K. and Virkar, A., Phase-stability, phase-transformation kinetics, and conductivity of Y_2O_3–Bi_2O_3 solid electrolytes containing aliovalent dopants. *Journal of the American Ceramic Society*, 1991, **74**(8), 1970–1980.
78. Keizer, K., Verkerk, M. J. and Burggraaf, A. J., Preparation and properties of new oxygen ion conductors for use at low temperatures. *Ceramurgia International*, 1979, **5**, 143–147.
79. Keizer, K., Burggraaf, A. J. and deWith, G., The effect of Bi_2O_3 on the electrical and mechanical properties of ZrO_2–Y_2O_3 ceramics. *Journal of Materials Science*, 1982, **17**, 1095–1102.
80. Winnubst, A. J. A. and Burggraaf, A. J., Preparation and electrical properties of a monophasic ZrO_2–Y_2O_3–Bi_2O_3 solid electrolyte. *Materials Research Bulletin*, 1984, **19**, 613–619.
81. Miyayama, M. and Yanagida, H., Oxygen ion conduction in fcc Bi_2O_3 doped with ZrO_2 and Y_2O_3. *Materials Research Bulletin*, 1986, **21**, 1215–1222.
82. Miyayama, M., Nishi, T. and Yanagida, H., Oxygen ionic conduction in Y_2O_3-stabilized Bi_2O_3 and ZrO_2 composites. *Journal of Materials Science*, 1987, **22**, 2624–2628.
83. Verkerk, M. J. and Burggraaf, A. J., High oxygen ion conduction in sintered oxides of the Bi_2O_3–Dy_2O_3 system. *Journal of the Electrochemical Society*, 1981, **128**, 75–82.
84. Verkerk, M. J., Keizer, K. and Burggraaf, A. J., High oxygen ion conduction in sintered oxides of the bismuth oxide–erbium oxide system. *Journal of Applied Electrochemistry*, 1980, **10**, 81–90.
85. Keizer, K., Verkerk, M. J. and Burggraaf, A. J., Preparation and properties of new oxygen ion conductors of the bismuth oxide–erbium oxide system. *Ceramurgia International*, 1979, **5**, 143–147.
86. Nasanova, S. N., Serbrennikov, V. V. and Natenov, G.A., Preparation and some properties of rare earth bismuthites. *Zhurnal Neoroganicheskoi Khimii*, 1973, **18**, 2350–2353.
87. Bouwmeester, H. J. M., Kruidhof, H., Burggraaf, A. J. and Gellings, P. J., Oxygen semipermeability of erbia-stabilized bismuth oxide. *Solid State Ionics*, 1992, **53–56**, 460–468.
88. VerKerk, M. J., Hammink, M. W. J. and Burggraaf, A. J., Oxygen transfer on substituted ZrO_2, Bi_2O_3, and CeO_2 electrolytes with platinum electrodes. *Journal of the Electrochemistry Society*, 1983, **130**(1), 70–78.
89. Nagamoto, H. and Inoue, H., Characteristics of electrode overpotential over doped bismuth oxide electrolyte. *Journal of the Electrochemical Society*, 1989, **136**(7), 2088–2093.
90. Verkerk, M. J., van De Velde, G. M. H., Burggraaf, A. J. and Helmholdt, R. B., Structure and ionic conductivity of bismuth sesquioxide substituted with lanthanide oxides. *Journal of the Physics and Chemistry of Solids*, 1982, **43**(12), 1129–1136.
91. Vinke, I. C., Seshan, K., Boukamp, B. A., DeVries, K. J. and Burggraaf, A. J., Electrochemical properties of stabilized δ-Bi_2O_3. Oxygen pump properties of Bi_2O_3–Er_2O_3 solid solutions. *Solid State Ionics*, 1989, **34**, 235–242.
92. Vinke, I. C., Bakiewicz, J. L., Boukamp, B. A., DeVries, K. J. and Burggraaf, A. J., Oxygen transport and transfer properties of erbia-stabilized bismuth oxide. *Solid State Ionics*, 1990, **40/41**, 886–888.
93. Vinke, I. C., Boukamp, B. A., de Vries, K. J. and Burggraaf, A. J., Three-electrode current-voltage measurements on ebia-stabilized bismuth oxide with sputtered noble mental electrodes. *Solid State Ionics*, 1992, **51**, 249–259.
94. Kruidhof, H., van de Velde, G. M. H., Seshan, K., de Vries, K. J. and Burggraaf, A. J., Bismuth oxide based ceramics with improved electrical and mechanical-properties. 2. Structural and mechanical-properties. *Materials Research Bulletin*, 1988, **23**, 371–377.
95. Kruidhof, H., Boumeester, H. J. M., de Vries, K. J., Gellings, P. J. and Burggraaf, A. J., Thermochemical stability and nonstiochiometry of erbia-stabilized bismuth oxide. *Solid State Ionics*, 1992, **50**, 181–186.
96. Battle, P. D., Catlow, C. R. A. and Moroney, L. M., Structual and dynamical studies of δ–Bi_2O_3 oxide–ion conductors. *Journal of Solid State Chemistry*, 1987, **67**, 42–50.
97. Battle, P. D., Hu, G., Moroney, L. M. and Munro, D. C., Structual and dynamical studies of δ-Bi_2O_3 oxide ion conductors. *Journal of Solid State Chemistry*, 1987, **69**, 30–35.
98. Barker, W. W., Graham, J., Parks, T. C. and Speed, T. P., Electrostatic energy of disorded distributions of vacancies or altervalent ions. *Journal of Solid State Chemistry*, 1977, **22**, 321–329.
99. Cahen, H. T., Van Den Belt, T. G. M., De Wit, J. H. W. and Broers, G. H. J., The electrical conductivity of δ-Bi_2O_3 stabilized by isovalent rare-earth oxides R_2O_3. *Solid State Ionics*, 1980, **1**, 411–423.
100. Mercurio, D., El Farissi, M., Frit, B., Reau, J. M. and Senegas, J., Fast ionic conduction in new oxide materials of the Bi_2O_3–Ln_2O_3–TeO_2 systems (Ln = La, Sm, Gd, Er). *Solid State Ionics*, 1990, **39**, 297–304.
101. Mercurio, D., El Farissi, M., Champarnaud-Mesjard, J. C., Frit, B., Conflant, P. and Roult, G., Structural study of the mixed-oxide $Bi_{0.7}La_{0.3}O_{1.5}$ using single-crystal x-ray-diffraction and powder neutron-diffraction. *Journal of Solid State Chemistry*, 1989, **80**, 133–143.
102. Verkerk, M. J. and Burggraaf, A. J., High oxygen ion conduction in sintered oxides of the bismuth oxide–dysprosium oxide (Bi_2O_3–Dy_2O_3) system. *Journal of the Electrochemical Society*, 1981, **128**(1), 75–82.
103. Tare, V. B. and Schmalzried, H., Ion and electron conductivity of some rare earth oxides. *Zeitschrift fuer Physikalische Chemie, N.F.*, 1964, **43**, 30–32.
104. Watanabe, A., Polymorphic transformation of δ-Bi_2O_3 stabilized with Ln_2O_3 (Ln = Sm, Eu, Gd, Tb and Dy) into a new phase with a C-type rare-earth oxide-related structure. *Solid State Ionics*, 1995, **79**, 84–88.
105. Watanabe, A., Preparation of a new phase having a cation-ordered C-type rare-earth oxide related structure in the systems Bi_2O_3–Ln_2O_3 (Ln = Sm, Eu, Gd, Tb, and Dy). *Journal of Solid State Chemistry*, 1995, **120**, 32–37.
106. Koto, K., Mori, H. and Ito, Y., Oxygen disorder in the fluorite-type conductors $(Bi_2O_3)_{1-x}(Gd_2O_3)_x$ by X-ray and EXAFS analysis. *Solid State Inoics*, 1986, **18&19**, 720–724.
107. Esaka, T. and Iwahara, H., Oxide ion and electron mixed conduction in the flurite-type cubic solid solution in the system Bi_2O_3–$Tb_2O_{3.5}$. *Journal of Applied Electrochemistry*, 1985, **15**, 447–451.
108. Watanabe, A., Phase relations of hexagonal and cubic phases in holmia-doped bismuth sesquioxide, $Bi_{2-2x}Ho_{2x}O_3$($x = 0{\cdot}205$-$0{\cdot}245$. *Solid State Ionics*, 1989, **3**, 35–39.
109. Takahashi, T., Iwahara, H. and Esaka, T., High oxide ion conduction in sintered oxide of the system Bi_2O_3–M_2O_3. *Journal of the Electrochemistry Society*, 1977, **124**, 1563–1569.
110. Powers, V. J., Ph D. thesis, Ohio State University, 1989.
111. Smolyaninov, N. P. and Belyaev, I. N., Equilibrium phases in the system Bi_2O_3–V_2O_3–PbO. *Zhurnal Neorganicheskoi Khimii*, 1963, **8**, 1213–1223.
112. Panchenko, T. V., Katov, V. F., Kostyuk, V K h., Truseeva, N. A. and Shmal'ko, A. V., New bismuth-containing crystal $Bi_{14}V_4O_{31}$. *Ukainskii. Fizicheskii. Zhurnal*, 1983, **28**, 1091–1093.

113. Blinovskov, Ya. N. and Fotiev, A. A., Bismuth (3+) oxide–vanadium pentoxide system. *Zhurnal Neorganicheskoi Khimii*, 1987, **32**, 254–256.
114. Touboul, M. and Vachon, C., The Bi_2O_3–V_2O_5 system and crystal data about some bismuth vanadates. *Thermochimica Acta*, 1988, **133**, 61–66.
115. Zhou, W., Defect fluorite-related superstructures in the Bi_2O_3–V_2O_5 system. *Journal of Solid State Chemistry*, 1988, **76**, 904–300.
116. Zhou, W., The type-II superstructural family in the Bi_2O_3–V_2O_5 system. *Journal of Solid State Chemistry*, 1990, **87**, 44–54.
117. Kashida, S. and Hori, T., X-ray study of the cation distribution in the ternary oxide, $6Bi_2O_3$-V_2O_5. *Journal of Solid State Chemistry*, 1996, **122**, 358–363.
118. Watanabe , A., $Bi_{23}M_4O_{44.5}$ (M = P and V) —new oxide-ion conductors with triclinic structure based on a pseudo-fcc subcell, *Solid State Ionics*, 1997, **75**, 81–96.
119. Lu, T. and Steele, B. C. H., Electrical Conductivity of polycrystalline $BiVO_4$ samples having the scheelite structure. *Solid State Ionics*, 1986, **21**, 339–342 .
120. Debreuille-Gresse, M. F., Ph.D. thesis, The University of Lille, 1986.
121. Sleight, A. W., Chen, H. Y., Ferretti, A. and Cox, D. E., Crystal growth and structure of bismuth vanadate ($BiVO_4$). *Materials Research Bulletin*, 1979, **14**, 1571–1581.
122. David, W. I. F., Glazer, A. M. and Hewat, A. W., The structure and ferroelastic phase transition of bismuth vanadate ($BiVO_4$). *Phase Transitions*, 1979, **1**, 155–169.
123. Pinczuk, A., Welber, B. and Dacol, F. H., Mechanism of the ferroelastic transition of bismuth vanadate. *Solid State Communications*, 1979, **29**, 515–518.
124. Ramadass, N., Palanisamy, T., Gopalakrishnan, J., Aravamudan, G. and Sastri, M. V. C., Some ABO_3 oxides with defect pyrochlore structure. *Solid State Communications*, 1975, **17**, 545–547.
125. Vinke, I. C., Diepgrond, J., Boukamp, B. A., DeVries, K. J. and Burggraaf, A. J., Bulk and electrochemical properties of $BiVO_4$. *Solid State Ionics*, 1992, **57**, 83–89.
126. Boukamp, B. A., van Dijk, M. P., DeVries, K. J. and Burggraaf, A. J., Electrochemical properties of non-stoichiometric solid oxides. *Advanced Ceramics*, 1987, **23**, 445–453.
127. Burggraaf, A. J., Boukamp, B. A., Vinke, I. C. and De Vries, K. J., In *Advances in Solid State Chemistry*, vol. 1, ed. C. R. A. Catlow, JAI Press, London, 1989, p 259.
128. Abraham, F., Debreuille-Gresse, M. F., Mairesse, G. and Nowogrocki, G., Phase transitions and ionic conductivity in $Bi_4V_2O_{11}$ an oxide with a layered structure. *Solid State Ionics*, 1988, **28–30**, 529–532.
129. Abraham, F., Boivin, J. C., Mairesse, G. and Nowogrocki, G., The BIMEVOX series: a new family of high performance oxide ion conductors. *Solid State Ionics*, 1990, **40/41**, 934–937.
130. Aurivillius, B., Mixed bismuth oxides with layer lattices I. Structure type of $CaCb_2Bi_2O_9$. *Arkiv. Kemi.*, 1949, **1**, 463–480.
131. Lee, C. K., Sinclair, D. C. and West, A. R., Stoichiometry and stability of bismuth vanadate, $Bi_4V_2O_{11}$, solid solutions. *Solid State Ionics*, 1993, **62**, 193–198.
132. Iharada, T., Hammouche, A., Foultier, J., Kleitz, M., Boivin, J. C. and Mairesse, G., Electrochemical characterization of BIMEVOX oxide-ion conductors. *Solid State Ionics*, 1991, **48**, 257–265.
133. Reiselhuber, K., Dorner, G. and Breiter, M. W., Studies of BICUVOX.10 by conductivity measurements and differential thermal analysis. *Electrochimica Acta*, 1993, **38**, 969–973.
134. Anne, M., Bacmann, M., Pernot, E., Abraham, F., Mairesse, G. and Strobel, P., Stucture of new anionic conductors $Bi_4V_{2(1-x)}M_{2x}O_{11-3x}$, M = Cu, Ni. *Physica B.*, 1992, **180–181**, 621–623.
135. Pernot, E., Anne, M., Bacmann, M., Strobel, P., Foultier, J., Vannier, R. N., Mairesse, G., Abraham, F. and Nowogrocki, G., Structure and conductivity of Cu and ni-substituted $Bi_4V_2O_{11}$ compounds. *Solid State Ionics*, 1994, **70/71**, 259–263.
136. Francklin, A. J., Chadwick, A. V. and Couves, J. W., Thermoelectric power studies of bismuth based oxides. *Solid State Ionics*, 1994, **70/71**, 215–220.
137. Sharma, V., Shukla, A. K. and Gopalakrishnan, J., Effect of aliovalent-cation substitution on the oxygen–ion conductivity of $Bi_4V_2O_{11}$. *Solid State Ionics*, 1992, **58**, 359–362.
138. Goodenough, J. B., Manthiram, A., Paranthaman, P. and Zhen, Y. S., Fast oxide-ion conduction in intergrowth structures. *Solid State Ionics*, 1992, **52**, 105–109.
139. Vannier, R. N., Mairesse, G., Abraham, F. and Nowogrocki, G., Incommensurate superlattice in Mo-substitued $Bi_4V_2O_{11}$. *Journal of Solid State Chemistry*, 1993, **103**, 441–446.
140. Vannier, R. N., Mairesse, G., Nowogrocki, G., Abraham, F. and Boivin, J. C., Electrical and structural investigations on a new bismuth lead vanadium oxide solid electrolyte. *Solid State Ionics*, 1992, **53–56**, 713–722.
141. Vannier, R. N., Mairesse, G., Abraham, F. and Nowogrocki, G., Double substitutions in $Bi_4V_2O_{11}$. *Solid State Ionics*, 1994, **70/71**, 248–252.
142. Joubert, O., Ganne, M., Vannier, RN. and Mairesse, G., Solid phase synthesis and characterization of new BIMEVOX series: $Bi_4V_{2-x}M_xO_{11-x}$(M = Cr^{III}, Fe^{III}). *Solid State Ionics*, 1996, **83**, 199–207.
143. Lazure, S., Vernochet, Ch., Vannier, R. N., Nowogrocki, G. and Mairesse, G., Composition dependence of oxide anion conduction in the BIMEVOX family. *Solid State Ionics*, 1996, **90**, 117–123.
144. Abrahams, I., Krok, F. and Nelstrop, J. A. G., Defect structure of quenched γ-BICOVOX by combined X-ray and neutron powder diffraction. *Solid State Ionics*, 1996, **90**, 57–65.
145. Krok, F., Abrahams, I., Bangobango, D. G., Bogusz, W. and Nelstrop, J. A. G., Electrical and structural study of BICOVOX. *Solid State Ionics*, 1996, **86–88**, 261–266.
146. Krok, F., Bogusz, W., Jakubowski, W., Dygas, J. R. and Bangobango, D., Studies on preparation and electrical conductivity of BICOVOX. *Solid State Ionics*, 1994, **70/71**, 211–214.
147. Kurek, P. and Breiter, M. W., Thermal stability and ionic conductivity of the BIMEVOX.10 ceramic (ME = Zn, Ni). *Solid State Ionics*, 1996, **86–88**, 131–135.
148. Lee, C. K. and West, A. R., Thermal behavior and polymorphism of BIMEVOX oxide ion conductors including the new materials: $Bi_4V_2O_{11}$:M:M = La, Y, Mg, B. *Solid State Ionics*, 1996, **86–88**, 235–239.
149. Joubert, O., Jouanneaux, A., Ganne, M., Vannier, R. N. and Mairesse, G., Solid phase synthesis and characterisation of new BIMEVOX series: $Bi_4V_{2-x}M_xO_{11-x/2}$ (M = Sb^v, Nb^v).. *Solid State Ionics*, 1994, **73**, 309–318.
150. Yan, J. and Greenblatt, M., Ionic conductivities of $Bi_4V_{2-x}M_xO_{11-x/2}$(M = Ti, Zr, Sn, Pb). *Solid State Ionics*, 1995, **81**, 225–233.
151. Vannier, R. N., Mairesse, G., Abraham, F. and Nowogrocki, G., Incommensurate superlattice in Mo-substituted $Bi_4V_2O_{11}$. *Journal of Solid State Chemistry*, 1993, **103**, 441–446.
152. Thery, O., Vannier, R. N., Dion, C. and Abraham, F., Preparation, characterization and oxide ion conductivity in U-substituted $Bi_4V_2O_{11}$. *Solid State Ionics*, 1996, **90**, 105–110.
153. Boivin, J. C. and Thomas, D. J., Structural investigations on bismuth-based mixed oxides. *Solid State Ionics*, 1981, **3/4**, 457–462.
154. Conflant, P., Boivin, J. C. and Thomas, D., Le diaggramme des phases solides du systéme Bi_2O_3–CaO. *Journal of Solid State Chemistry*, 1976, **18**, 133–140.

155. Guillermo, R., Conflant, P., Boivin, J. C. and Thomas, D., Le diagramme des phases du système Bi_2O_3-SrO. *Revue de Chimie Minérale*, 1978, **15**, 153–159.
156. Boivin, J. C. and Thomas, D. J., Crystal chemistry and electrical properties of bismuth-based mixed oxides. *Solid State Ionics*, 1981, **5**, 523–526.
157. Conflant, P., Boivin, J. C., Nowogocki, G. and Thomas, D., Etude structure par diffractometrie X A haute temperature du conducteur anionique $Bi_{0.844}Ba_{0.156}O_{1.422}$. *Solid State Ionics*, 1983, **9&10**, 925–928.
158. Suzuki, T., Yamazaki, T., Kaku, K. and Ikegami, M., An application of oxide and silver electrode on the barium oxide-doped bismuth oxide (Bi_2O_3) electrolyte. *Solid State Ionics*, 1985, **15**, 241–2146.
159. Sillen, L. G. and Aurivillius, B., Oxide phases with a defect oxygen lattice. *Zeitschrift für Kristallographie*, 1939, **101**, 483–495.
160. Suzuki, T., Dansui, Y., Shirai, T. and Tsubaki, C., Defect structure and electrical conductivity in rapidly-quenched and slowly-cooled rhombohedral solid solutions of the system bismuth (III) oxide–barium oxide. *Journal of Materials Science*, 1985, **20**, 3125–3130.
161. Biefeld, R. M. and White, S. S., Temperature/composition phase diagram of the system Bi_2O_3–PbO. *Journal of the American Ceramic Society*, 1981, **64**, 182–184.
162. Aurivillius, R. and Sillen, L. G., Polymorphy of bismuth trioxide. *Nature*, 1945, **155**, 305–306.
163. Boivin, J. C., Thomas, D. and Tridot, G., Contribution à l'étude du système de bismuth–oxide de plomb. *Comptus Rendus Academe Sciences Paris, Series C*, 1969, **268**, 1149–1151.
164. Boivin, J. and Tridot, G., Les phases solides du systéme Bi_2O_3–PbO: identification et évolution en fonction de la température. *Comptus Rendus Academe Sciences Paris, Series C*, 1974, **278**, 865–867.
165. Sammes, N. M., Tompsett, G. and Cartner, A. M., Characterization of bismuth lead oxide by vibrational spectroscopy. *Journal of Materials Science*, 1995, **30**, 4299–4308.
166. Honnart, F., Boivin, J. C., Thomas, D. and DeVries, K. J., Bismuth–lead oxide, a new highly conductive oxygen material. *Solid State Ionics*, 1983, **9&10**, 921–924.
167. Boivin, J. C., These d'Etat, Lille, 1975.
168. Demonchy, P., Boivin, J. C. and Thomas, D., Mesures de conductivité dans le système Bi_2O_3–PbO par la méthode des impédances complexes. *Comptus Rendus Academe Sciences Paris, Series C*, 1980, **290**, 279–282.
169. Sammes, N. M., Philips, R. J. and Fee, M. G., Phase stability and ionic conductivity in bismuth lead (antimony) oxide. *Solid State Ionics*, 1994, **69**, 121–126.
170. Sammes, N. M., Phillips, R. J., Fee, M. G. and Ratnaraj, R., Improved mechanical properties of bismuth lead oxide. *Journal of Materials Science Letters*, 1994, **13**, 1395–1396.
171. Fee, M. G., Sammes, N. M., Tompsett, G., Soto, T. and Cartner, A. M., The effect of heat treatment on the physical and electrical properties of the fast ion conductor $Bi_8Pb_5O_{17}$. *Solid State Ionics*, 1997, **95**, 183–189.
172. Sammes, N. M., Tompsett, G. and Cartner, A. M., High temperature Raman spectra of $Bi_8Pb_5O_{17}$. *Solid State Communications*, 1995, **96**, 545–548.
173. Sammes, N. M., Tompsett, G., Phillips, R., Carson, C., Cartner, A. M., Fee, M. G. and Yamamoto, O., Characterisation and stability of the fast ion conductor $(Bi_2O_3)_{1-x}(PbO)_x$. *Solid State Ionics*, 1996, **86–88**, 125–130.
174. Sammes, N. M., Du, Y. and Tompsett, G. A., Effect of Sb_2O_3 dopant concentration on the phase equilibria and stability of $Bi_8Pb_5O_{17}$. In *SOFC V*, ed. U. Stimming, S. C. Singhal, H. Tagawa and W. Lehnert, 1997, pp. 1051–1056.
175. Du, Y., Sammes, N. M., Tompsett, G. and Zhang, Y., Phase equilibria of bismuth lead antimony oxide. *Solid State Ionics*, 1999, in press.
176. Dumélié, M., Nowogrocki, G. and Boivin, J. C, Ionic conductor membrane for oxygen separation. *Solid State Ionics*, 1988, **28–30**, 524–528.
177. Fee, M. G. and Long, N. J., Mixed conductivity in metal-doped bismuth–lead oxide. *Solid State Ionics*, 1996, **86–88**, 733–737.
178. Bettahar, N., Conflant, P., Boivin, J. C., Abraham, F. and Thomas, D., Electrical conductivity of $(Bi,Pb)_2MO_4$ (M = Pd, Pt) linear chain compounds. *Journal of Physics and Chemistry of Solids*, 1985, **46**, 297–299.
179. Omari, M., Drache, M., Conflant, P. and Boivin, J. C, Anionic condtion properties of the fluorite-type phase in the Bi_2O_3–Y_2O_3-PbO system. *Solid State Ionics*, 1990, **40/41**, 929–933.
180. Drache, M., Conflant, P. and Boivin, J. C., Anoinic conduction properties of Bi–Ca–Pb mixed oxides. *Solid State Ionics*, 1992, **57**, 245–249.
181. Takahashi, T., Esaka, T. and Iwahara, H., Oxide ion conduction in the sintered oxides of MoO_3-doped Bi_2O_3. *Journal of Applied Electrochemistry*, 1977, **7**, 31–35.
182. Susuki, T., Kaku, K., Ukawa, S. and Dansui, Y., Low-temperature performance of thin solid electrolyte cell based on MoO_3-doped Bi_2O_3. *Solid State Ionics*, 1984, **13**, 237–239.
183. Boon, L. and Metselaar, R., Transport properties of $Bi_6Mo_2O_{15}$. *Solid State Ionics*, 1985, **16**, 201–210.
184. Hoda, S. N. and Chang, L. L. Y., Phase relations in the system bismuth (III) oxide–tungsten (VI) oxide. *Journal of the American Ceramic Society*, 1974, **57**, 323–326.
185. Watanabe, A., Ishizawa, N. and Kato, M., An outline of the structure of $7Bi_2O_3{\cdot}2WO_3$ and its solid solution. *Solid State Chemistry*, 1985, **60**, 252–257.
186. Esaka, T., Iwahara, H. and Kunieda, H., Oxide ion and electron mixed conduction in sintered oxides of the system Bi_2O_3–Pr_6O_{11}. *Journal of Applied Electrochemistry*, 1982, **12**, 235–240.
187. Sammes, N. M. and Gainsford, G. J., Phase stability and oxygen ion conduction in Bi_2O_3–Pr_6O_{11}. *Solid State Ionics*, 1993, **62**, 179–184.
188. Shuk, P., Jacobs, S. and Mobius, H. H., Mischassen des Bismuthtoxids mit terbium-und praseodymiumoxid. *Zeitschrift für Anorganishe und Allgemeine Chemie*, 1985, **524**, 144–156.
189. Esaka, T., Mangahara, T. and Iwahara, H., Oxide ion conduction in the sintered oxides of the system Bi_2O_3-MO_2(M = Ti, Sn, Zr, Te). *Solid State Ionics*, 1989, **36**, 129–132.
190. Fries, T., Lang, G. and Kemmler-Sack, S., Defect flourite structures in the Bi-rich part of the system Bi_2O_3–Re_2O_7. *Solid State Ionics*, 1996, **89**, 233–240.